HyMoCARES Project
WPT3. EFFECTS OF HYDROMORPHOLOGICAL MANAGEMENT AND RESTORATION MEASURES
D.T3.3.1 Technical note on the evaluation of physical and ecological effects of river restoration works

Case studies: Drau, Mur, Salzach (Austria)

Project: HyMoCARES
Work package: WPT3. Effects of hydromorphological management and restoration measures
Activity: A.T3.2-3. Evaluating physical and ecological effects of management/restoration works
Deliverable: D.T3.3.1. Technical notes on the evaluation of physical and ecological effects of river restoration works
Status: final
Date: 24-10-2019
Authors: Mario Klösch, Roman Dunst, Sebastian Pessenlehner, Ursula Stephan, Rolf Rindler, Philipp Gmeiner, Helmut Habersack
Revision:
Approval: PP10 Irstea

This project is co-financed by the European Regional Development Fund through the Interreg Alpine Space programme

www.alpine-space.eu/hymocares

This project is co-financed by the European Regional Development Fund through the Interreg Alpine Space programme

www.alpine-space.eu/hymocares

CONTENTS

1 Introduction

1.1 Drau River

The study site at the Austrian Drau River is located in the Upper Drau valley in the South of Austria in the region of Carinthia with the main focus on two restored reaches near the villages of Kleblach (Figure 1a) and Obergottesfeld. This area is part of the Austrian Alps; elevations reach from around 550 m up to more than 3000 m. The catchment basin drains around 2445 km² and covers parts of the southern limestone Alps as well as east alpine crystalline. The dominant sediment is gravel with a median diameter (d_{50}) of 25 mm. Sediment input mainly results from upstream active torrents in the catchment. The channel slope at the study site is approximately 0.002. The mean discharge is about 74 m³/s; a one-year flood reaches 320m³/s. Floods mostly occur in spring when snowmelt – and also glacier melt - is released into the basin, or in summer after thunderstorms. The discharge regime can be described as strongly pronounced nivo-glacial with a maximum discharge in June (Mader, 1996). The mean annual rainfall in Sachsenburg (close to the study site) is around 982 mm/a (BMFLUW, 2014). Historically, the Drau River at the studied reach was a wandering river (Figure 1b), which results from a transition from a braided to a meandering morphology, before it was regulated and finally restored.

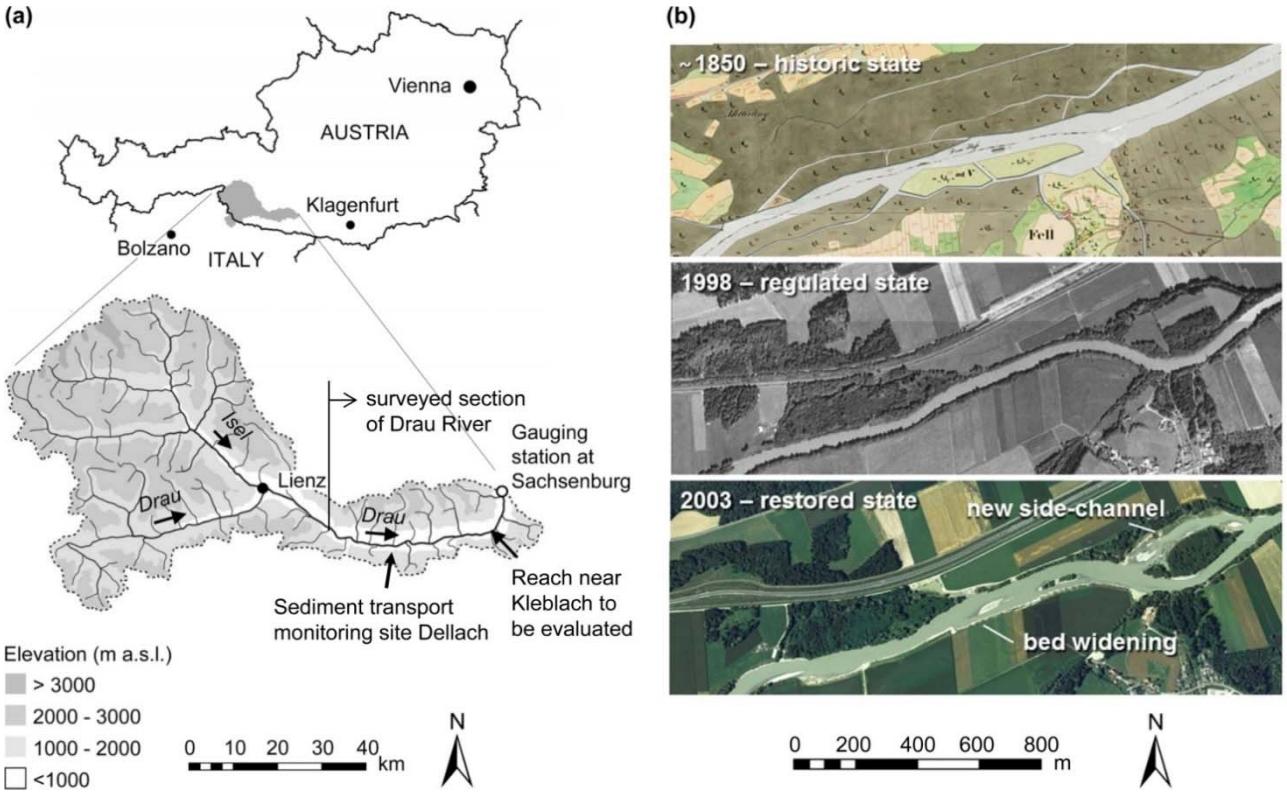

Figure 1. Drau River at Kleblach-Lind in the historic, regulated and restored state (Klösch and Habersack, 2017)

Several regulation measures (straightening, narrowing, riprap) were implemented in the late 19th century as well as in the 1960s. The resulting shear stress, in combination with reduced sediment input due to check dams, gravel mining and hydropower plants led to continued channel incision and alterations of habitats.
To counteract the trend of incision, several riverbed widenings were applied to stabilize the riverbed, improve flood protection by providing an appropriate channel width and to re-establish the ecological integrity of the river.

In the course of restoration works at the study site in Kleblach-Lind, the riverbed was widened and a side channel was excavated in order to provide space for self-dynamic widening (Figure 1b). In the side channel, groynes were embedded to prevent uncontrolled bank retreat. The whole restored reach is 1.8 km long

5 km downstream of Kleblach, near the village Obergottesfeld, another reach was restored. The restoration measures included the excavation of two side-channels, one 1 km in length, the other 600 m in length, and again an embedment of groynes. Finished in 2011, the upstream side-channel quickly widened and triggered massive bank retreat, which required the installation of additional groynes.

Figure 2. Emergence and enlargement of a mid-channel bar at a restored site of the Drau River, accompanied by excessive widening which required an expansion of bank protection (groynes) to prevent erosion of land outside of the provided corridor (source: Carinthian government).

1.2 Mur River

The study site at the Mur river is located near Gosdorf in Styria. There, the Mur represents the border between Austria and Slovenia along about 34 km. At the study site, the river length reaches 355 km with a catchment size of 10,340 km². The reach is characterized by a mean slope of 0.0014 and lies in a tertiary basin. The mean discharge is 150 m³/s, the 1-year flood event reaches 700 m³/s. The highest discharges occur during snowmelt in May; second flow peaks occur in July/ August. The hydrograph therefore is moderate nival (Mader et al., 1996). The Mur is a gravel bed river; at the border reach, the bed material has a mean diameter of approximately 35 mm. The mean annual rainfall in Unterpulka (close to the study site) is around 812 mm/a (BMFLUW, 2014). At the border reach, the Mur River was once a wandering/braided river system.

Due to missing sediment input upstream, degradation occurred along the whole reach of the River Mur over the last decades. In some locations, the riverbed elevation was up to 1.3 m lower than in 1970. Borehole drilling in one location revealed a thickness of the

gravel layer above the tertiary sediment of only 0.5 m, so that countermeasures were urgently needed to prevent a riverbed breakthrough (erosion into the finer grained tertiary sediment) or at least a loss of the gravel layer with its river functions and its role as a physical habitat component.

The Basic water management concept (Austrian-Slovenian Standing Committee for the Mur River, 2001) was developed, which recommended a series of counter measures. As recommended, a set of measures was implemented at Gosdorf (Figure 3) in 2006 and 2007, with the objectives to:

- Reduce the bedload transport capacity through self-dynamic widening and deceleration of the flow
- Provide bedload for the incised, downstream section by inducing bank erosion and by replenishing the sediment from a dredged side-channel into the main channel
- Establish a more diverse river geometry of higher ecological value

The measures were implemented over a length of 1 km and included the removal of bank protection structures along the Austrian riverbank, the excavation of a new side-channel, and the immediate insertion of the excavated sediment into the main channel (Figure 3). In the Basic Water management concept (Austrian-Slovenian Standing Committee for the Mur River, 2001), a sediment transport model was applied to test different scenarios of the sequence of measure implementation in the border section of the Mura River (30 km in length). At the measure Gosdorf, the widening was assumed to double the width of the river and to deliver a corresponding amount of bank-derived gravel into the river to supply the degraded, channelized section downstream of the widening. The measure implementations which were recommended based on the sediment transport model, strongly depended on the assumed bank retreat rates and channel widening.

The bank erosion is therefore a crucial process for the functioning of the measure and requires repeated monitoring. If the river again started to degrade, the erodibility of the tertiary sediment is crucial. Once the river incised quickly after a riverbed breakthrough, very large amounts of sediment would be needed for restoration with ecologically oriented measures. Both issues gained attention during the HyMoCARES project.

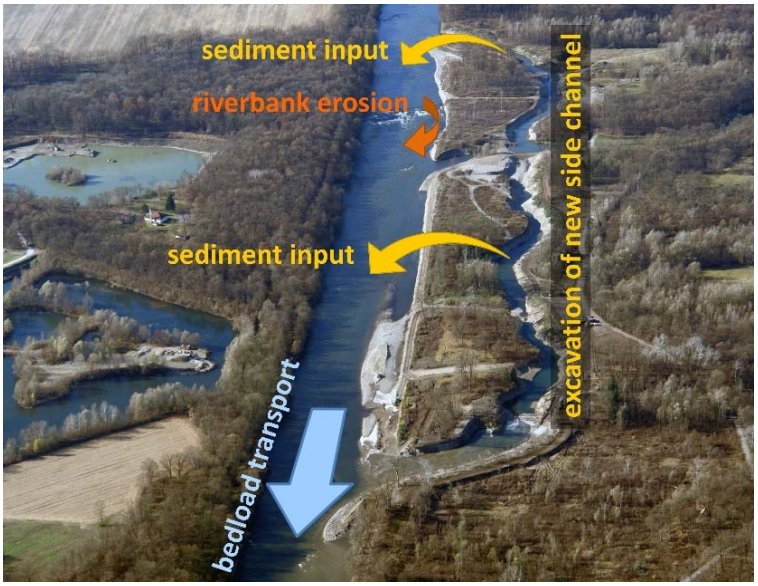

Figure 3. Implemented measures at Gosdorf (based on Klösch et al., 2011)

Figure 4 displays satellite images from the channelized (2004) and restored Mur section at Gosdorf.

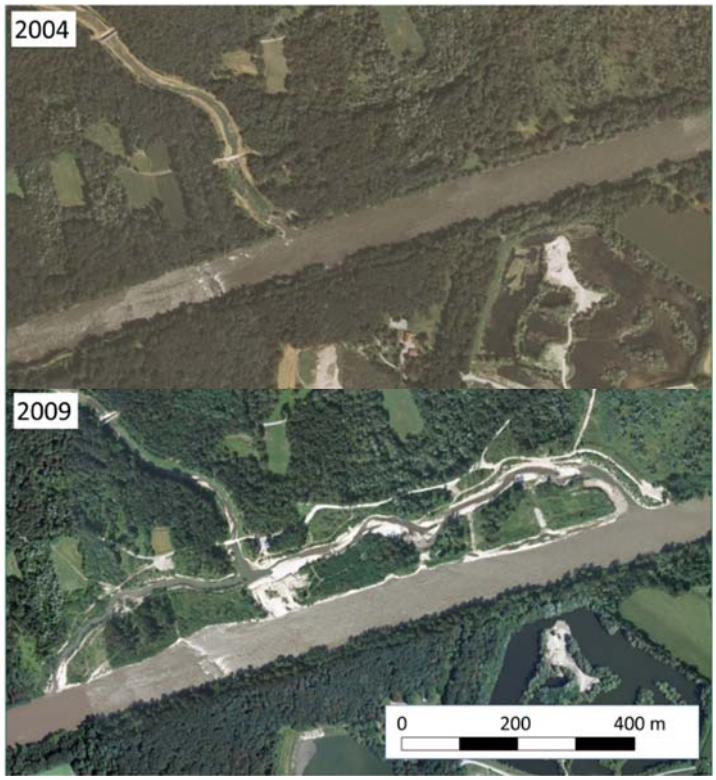

Figure 4. Mur River before (2004) and after (2009) restoration (image source: google earth)

1.3 Salzach River

The river Salzach leaves the northern eastern Alps near the town Salzburg and flows along the Austrian and Bavarian border through the Alpine foothills. The river has its source in the Kitzbühler Alpen/Österreich at a height of 2300 m a.s.l. and flows into the Inn (344 m a.s.l.); its total length is 225 km. In 1817 the river Salzach was a braided river. In the past 100 years, the river moved to a monotonous and straight river morphology due to various human activities such as width reduction, bed load retention in the upstream catchment and gravel extractions. As a consequence, a significant incision of the river bed (up to 5 meters in approximately 100 years) has been observed causing a significant lowering of the groundwater table. In addition, the risk of sudden river-bed break-through, especially during floods, increased as demonstrated by some events near Salzach (Amt der Salzburger Landesregierung 1969).

In 2010, a ramp was constructed at river-kilometer 51.9 to rise the bed level upstream (Figure 5). The ramp decreased the channel slope upstream and temporarily caused a trapping of the supplied sediment. To compensate the resulting temporary bedload deficit in the downstream section, the bank protection structures were removed in the downstream section. The gravel which enters the riverbed from bank erosion should compensate the deficit from upstream.

Figure 5. Step-pool ramp constructed in the year 2010 in the Salzach River to rise the bed level upstream. Removal of bank protection downstream intended to compensate the bedload deficit which resulted from sediment trapping upstream of the reservoir.

2 Monitoring approach

Due to availability of topographic data of the state before the restoration measures, the selected monitoring approach corresponds to a BA (Before-and-After) design.

2.1 Physical monitoring

2.1.1 Drau River

The monitoring activities at the Drau case study site addressed the long-term self dynamic morphologic evolution of the widened section near the village of Kleblach-Lind, the velocity of sediment transfer in the river channel, and a process study on bank erosion in the widening near the village of Obergottesfeld.

Morphological monitoring of the widening near Kleblach-Lind

At the Drau River, the widening near the village of Kleblach provided the possibility of analysing the longer time effects of channel widening on the sediment budget and the remaining morphodynamics after the rapid initial adjustments of channel morphology. Digital elevation models, which derived from surveys before and after measure implementation in 2002, allowed analysing the entire self-dynamic evolution including new surveys conducted within HyMoCARES. The morphological monitoring required the application of the following methods:

Main channel survey - During the course of the Project, the main channel at the study site Kleblach-Lind was surveyed in 2018 and 2019, using single-beam sonar. Using ArcGIS, the spatial data obtained was interpolated, considering break lines, to create Digital Elevation Models (DEM).

Side channel survey - Within the physical monitoring at the Drau River in Austria repeated UAV (unmanned aerial vehicle) surveys were conducted in the side channel (Figure 6d). For that purpose, a drone (Figure 6a) equipped with a camera was used to collect high-resolution spatial data in April 2017, April 2018 and March 2019. Structure from Motion (SfM) photogrammetry was applied to extract dense and accurate three-dimensional point clouds. The analysis of UAV-images was conducted with Agisoft PhotoScan Professional photogrammetric software. Submerged areas and areas covered by vegetation were additionally investigated by terrestrial surveying using a total station (Figure 6b). The data sets from the terrestrial survey and the drone survey were finally merged and Digital Elevation Models (DEM) for both measurement campaigns were derived and used to produce difference maps. The development of the elevation and the morphology respectively is crucial for the assessment of hydromorphological restoration measures.

Wolman pebble counts - To characterize the grain sizes in the monitored reach samples were taken using the Wolman pebble count technique (Wolman, 1954) (Figure 6c) in April 2017. A data set of 11 Wolman pebble counts was taken exposed and representative gravel bars. Each pebble count consisted of 100 grains collected along two lines. To minimize bias, all the grains were selected by the same person. A Pebble box (Bunte & Abt, 2001) was used to measure the b-axis of grains.

Figure 6. Morphological monitoring at the Drau River (Austria) – a) used drone for the structure from motion (SfM) photogrammetry, b) terrestrial survey, c) Wolman pebble counts for grain size analysis, d) location of the survey

Figure 7 shows the orthophoto of the drone survey 2017. The SfM-derived point clouds were georeferenced using 50 ground control points (Photogrammetry targets). The drone survey was complemented by a tachymetric survey of submerged or vegetated areas. The distribution of the ground control points, the tachymetric survey and the 11 Wolman Pebble Counts are visualised in Figure 7.

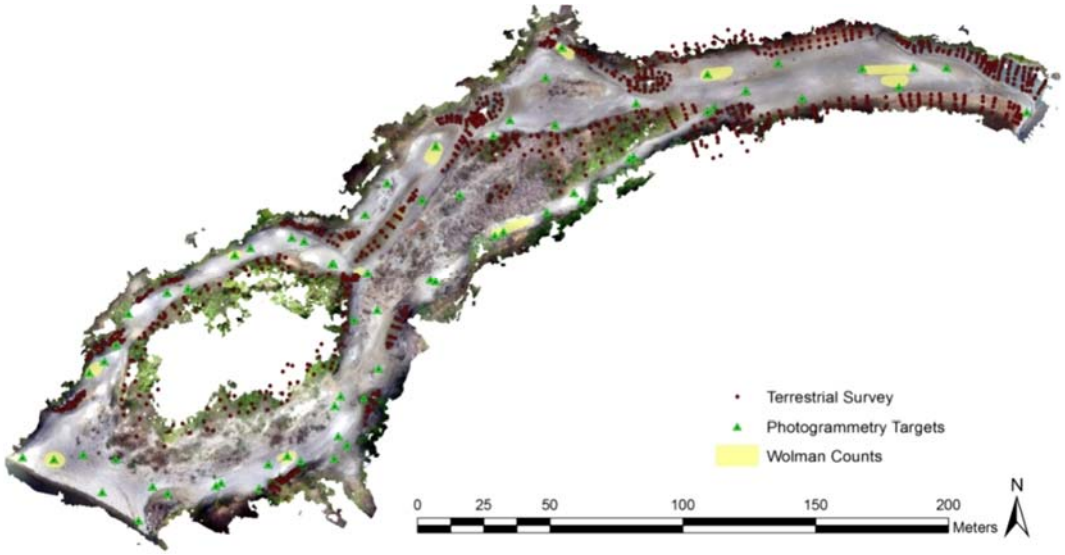

Figure 7 Orthophoto of the drone survey 2017 with location of the used ground control points (green triangle), terrestrial survey (red dots) and Wolman Pebble Counts (yellow areas)

According to Vázquez-Tarrío et al. (2017) a statistical analysis was used to link the detected roughness from the UAV-survey to the measured characteristic grain sizes of the pebble counts. For relating the grain sizes to the roughness of the point clouds different roughness descriptors were computed:

- (i) roughness height r_h (the difference in height between the top of the bed sediment and the locally averaged topographic surface)
- (ii) twice the standard deviation ($2\sigma z$) of elevations in a given area
- (iii) the root mean square height (RMSH), the standard deviation of heights in a given area for which the average slope has been detrended

The Software Cloud Compare was used for the calculation of the 3 different roughness metrics from the SfM point clouds. The calculated roughness values were compared with grain size percentiles to find the best grain size proxy. In a final step the derived rating curve was used to calculate grain size information of the whole side channel and analyse changes in the surface sediment.

Bedload tracer study on sediment transfer in the Upper Drau valley

A tracer study was conducted to investigate the velocity of bedload. The obtained data then served to derive a formula implemented in the tool SedRace (see deliverable D.T2.3.1), which helps practitioners to estimate the velocity of sediment transfer, e.g. following sediment replenishment actions. 65 coded radio transmitters were used to

create artificial stone tracers in 5 size classes using natural stones as templates (Figure 8a and Figure 8b). The artificial stones were selected based on a statistical analysis of the lengths of their three axes to identify stones with average axis relations. Around 20 km upstream of the study site Kleblach a sediment monitoring station of BOKU is located (Dellach im Drautal), which was equipped with a permanent logging antenna to detect the tracers passing by at this cross-section. The location of the antenna marked the downstream end of the investigated section and was installed to avoid the introduction of bias into the data analysis (following recommendations from Chapuis et al., 2014). The stone tracers were put into the Drau River during low flow conditions (~ 35 m^3/s) 5 km upstream of the antenna, assuming that this distance was sufficiently long for a monitoring duration of one year, so that most of the tracers remained in this section and that only a small part was transported further downstream crossing the antenna section. The survey of the tracer positions was performed from boat using a GPS-handheld, a receiver and an antenna (Figure 8c).

Figure 8. a) Original stones and tracer replications, b) All 65 coded radio tracer stones positioned next to the originals before insertion into the Drau River, and c) the process of searching the tracers by boat.

Continuous observation of bank erosion in the widening of Obergottesfeld

In the widened section near the village of Obergottesfeld time-lapse cameras were mounted (Figure 9) to assess the bank erosion which followed a major flood event (10 years return interval), to understand the processes leading to excessive widenings which occurred especially in this widened section.

Figure 9. Left: Localisation of the investigated riverbank and mid-channel bar section including direction of the cameras' view, right: Time-lapse cameras mounted on the Drau riverbank to continuously observe the occurring bank retreat

2.1.2 Mur River

Measuring riverbank retreat

The self-dynamic process of bank erosion was a crucial element of the pilot measure in Gosdorf, which should repeatedly deliver sediment into the channelized section downstream of Gosdorf, which suffered riverbed incision. To monitor the riverbank retreat, a terrestrial photogrammetry was conducted along the entire riverbank. The obtained data was then compared to the initial bank geometry directly after completion of the measures in 2007. The software Agisoft PhotoScan was used to obtain a dense point cloud from the photogrammetric images. The software ArcGIS was then used to interpolate DEMs of the present bank geometry, which could then be compared to the state in 2007.

Investigation of the tertiary sediment

At the border section of the Mur River, the possibility of a riverbed breakthrough during the next larger flood event is a realistic threat. If the gravel layer (quaternary sediment) is lost, the erodibility of the underlying tertiary sediment codetermines the incision rate which follows. The erosion rate ε due to fluvial erosion may be described by the following excess shear stress formula:

$$\varepsilon = k_d(\tau - \tau_c)$$

where τ is the shear stress, τ_c is the critical shear stress and k_d is the erodibility coefficient. The formula parameters τ_c and k_d were determined with the Jet-Test device (Figure 8), which applies a known shear stress at the sediment surface and allows repeated measurement of the resulting scour depth. The jet is submerged in water, so that the jet diameter increases and the shear stress decreases with distance to the jet nozzle.

Figure 10. Instrument setup at the Mur River for deploying the Jet-test device. a) Pump continuously delivering river water to the head tank, b) head tank with continuous overflow to ensure constant water pressure at the Jet-Test instrument, c) Jet-Test device mounted on the tertiary sediment, d) Jet exiting the nozzle (submerged in water during the experiment). The Jet-test device was provided by the U.S. Department of Agriculture, National Sedimentation Laboratory, Oxford, Mississippi.

2.1.1 Salzach River

At the Salzach River no new data was obtained within the project, but the tool Chevo, which was developed in HyMoCARES, was applied to existing cross section data from dates before (2005) and after (2015) the measure implementation (2010).

2.2 Ecological monitoring

2.2.1 Drau River case study

A three-year post-treatment monitoring was conducted in order to measure the success of the implemented restauration measures in the course of the LIFE Project. The monitoring program included fishing, transect mapping, mapping of spawning habitats.

2.2.2 Mur River case study

Within the EU Interreg SI-AT project DRA-MUR-CI the reach was monitored for fish species, the colonisation by wading birds and bank-nesting birds, reptiles, amphibians and vegetation, which included the colonisation by neophytes.

3 Physical effects

3.1 Drau River

3.1.1 Morphological evolution of the widening in Kleblach-Lind

The surveys allowed creating two DEMs of the entire widened section near Kleblach-Lind for spring 2018 and spring/summer 2019, so that the effects of a major flood with a 10-year recurrence interval in October 2018 could be fully captured. The data obtained in HyMoCARES enabled the continuation of a long series of channel surveys (Figure 11) and the analyses of morphologic changes.

A small flood with a peak discharge of 286 m^3/s in the first year after channel construction almost doubled the mean width of the side channel from 29 m to 55 m. Widening was largest upstream, where it was accompanied by the development of a large mid-channel bar. The groynes along the left bank were exposed quickly by bank erosion and have since then acted as constraints to the channel morphology. Due to aggradation the side-channel disconnected at low flow conditions, so that the inlet was modified in 2009 (the inlet structure - kind of a groyne - was set back a few meters). In the main channel the bed-levels rose after the implementation of the restoration measure. More diverse flow patterns were established and habitats were successfully recreated. Large bars developed, but they are immobile given the remained channel constraints and continue aggrading. This aggrading trend continued until 2018. However, a re-initiation of morphodynamics resulted from the 10-years-flood in October 2018, where the river partly destroyed artificial channel constraints and where the river adjusted to another widening measure which was implemented in 2014.

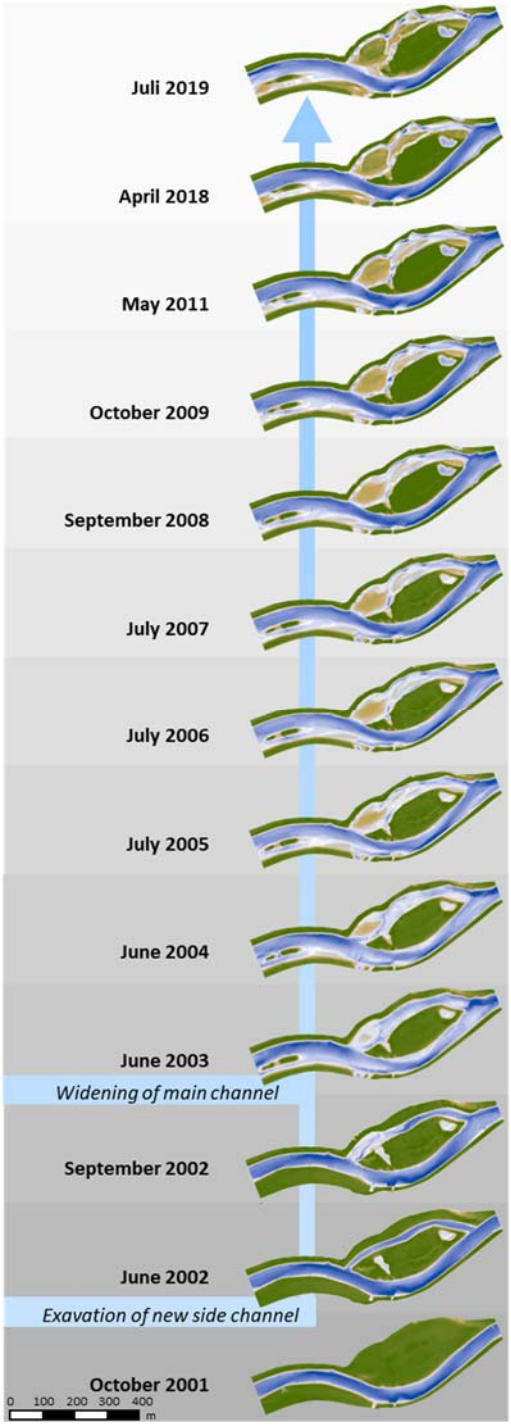

Figure 11. Change of morphology after the excavation of a new side channel in 2002 and the widening of the main channel in 2003 (Habersack et al., 2013). The elevation was detrended based on the valley slope, so that the colours approximately represent a relative elevation to the water surface. The white contours approximately represent the position of the water edge.

Figure 12 displays DEMs with detrended elevation for the state in 2018 (before the flood) and 2019. To quantify the changes, DEMs of difference were calculated, subtracting 2018 from 2019, using the outlines of the riverbed of 2018 (Figure 13a) and the riverbed of 2018 plus a 30m buffer (Figure 13b), in order to take into account the bank erosion.

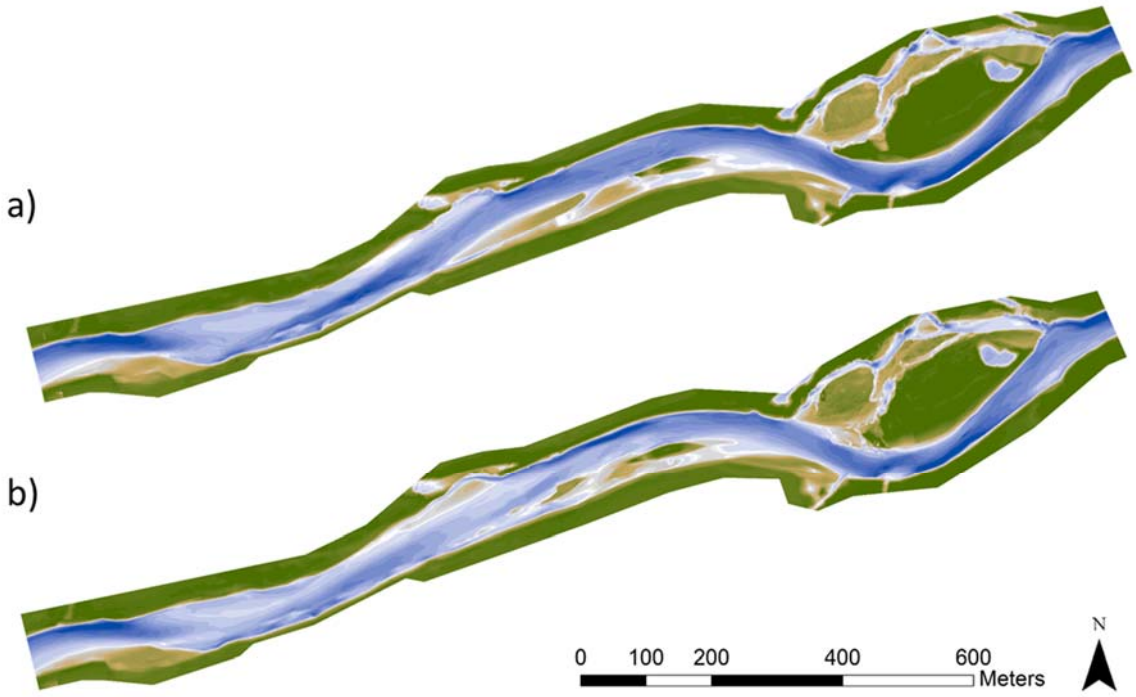

Figure 12. Detrended DEM 2018 (a) and 2019 (b)

Figure 13 shows the morphodynamic changes in this time period. A widening which was implemented by excavation in 2014 on the right side between km 35.8 and km 36.1 can be suggested to be the main cause for significant changes in the section directly downstream, where a large, vegetated bar was strongly reduced in size. At the same time, the bed levels next to the former bar position rose and another bar strongly enlarged in size (km 36.2).

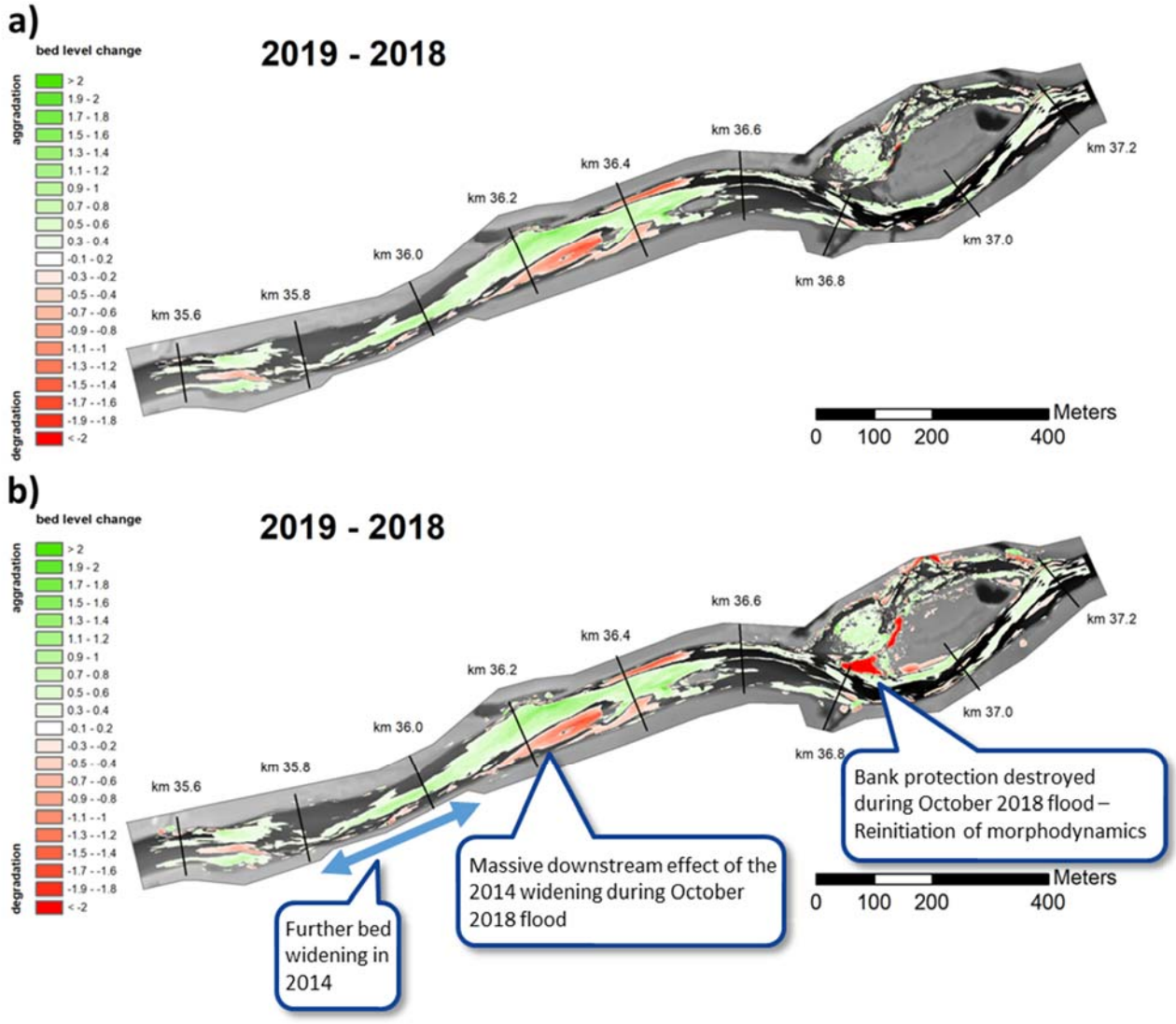

Figure 13. Difference map - DEM 2019 minus DEM 2018; (a) with and (b) without bank erosion considered; red: erosion, green: aggradation

At the right side of the inlet of the side channel the flood at the end of October eroded up to 50m of the tip of the island at km 36.8 (Figure 13b), which the side channel after destroying the bank protection at the right channel inlet. This change of boundary conditions led to changes in morphology (e.g. right riverbank further downstream the side channel).

In this time span between spring 2018 and spring/summer 2019, roughly 20,000 m^3 were deposited on the river bed (the analysis was restricted to the area of the formerly channelized bed). Figure 14 shows continuous aggradation in the entire main channel, except for some limited degradation at km 36.3 given the re-initiation of morphodynamics by excessive erosion of the deposited bar. The sediment volume which deposited as a result of the flood in October is remarkable portion of the total sediment volume (about 45,000 m^3) which was deposited in the entire period since the implementation of the widening measures.

The effect of bank erosion was not considered in the sediment budget analysis, as the analysis was restricted to the area of the former main channel bed. Performing the analysis in the area of the widened riverbed of 2003, 18530m^3 of sediment were deposited during the period from 2018 to 2019, of which 3050m^3 were deposited in the side channel.

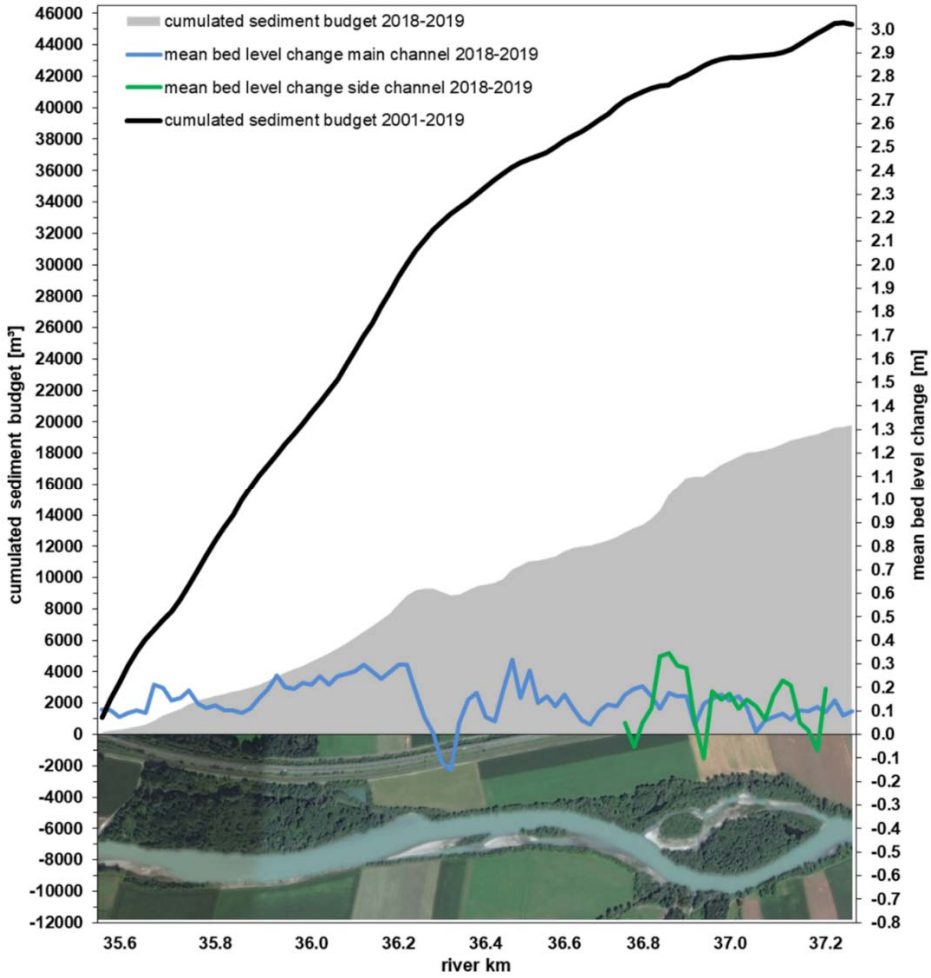

Figure 14. Cumulated sediment budgets in the area of the formerly channelized river.

Figure 15 shows DEMs of difference (DoD) of the channel evolution between 2001 and 2019 (Figure 15a), which is restricted to the area of the formerly regulated riverbed, and between 2003 and 2019 (Figure 15b) in the widened riverbed of 2003 after measure implementation.

Figure 15a reproduces the dominance of bed aggradation in the entire reach, with highest aggradation upstream, which indicates an adjustment of channel slope to re-establish transport capacity. Compared to Figure 15a, Figure 15b (difference between 2019 and 2003) shows a degradation in the main channel between km 36.7 to km 37.2. This degradation followed the initial aggradation in the main channel, which occurred at the time after the initial self-dynamic widening of the side-channel. At that time, the transport capacity in the main channel was strongly reduced as the side channel carried a considerable portion of the discharge in 2003 (the side channel could carry 33% of a

bankfull discharge according to Formann et al., 2007). Bar growth in the side-channel then again reduced the side-channel discharge, the hydraulic load in the main channel increased again and eroded the sediment which was at first deposited.

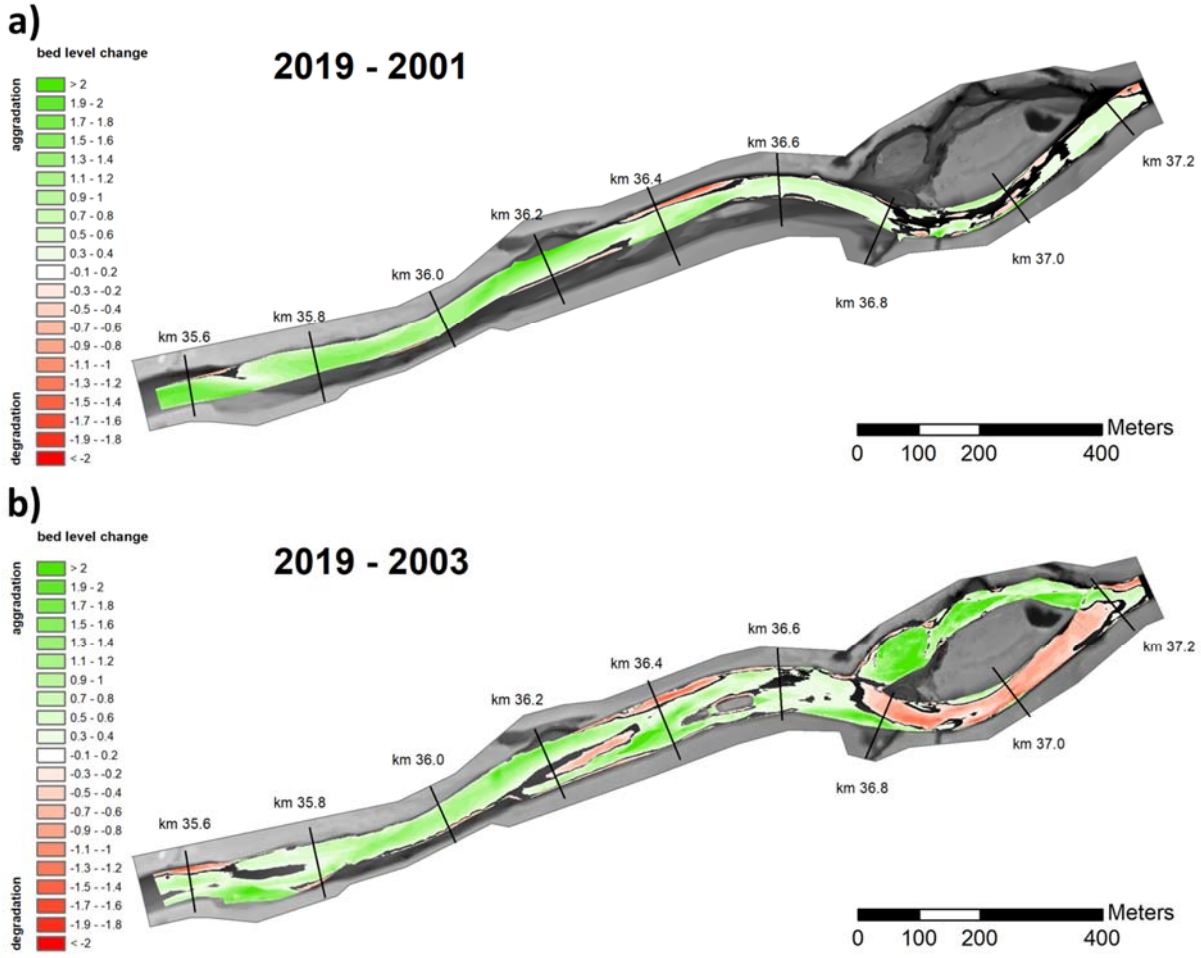

Figure 15. Difference maps: a) DEM 2019 minus DEM 2001 in the channelized riverbed of 2001, b) DEM 2019 minus DEM 2003 in the widened riverbed of 2003.

Figure 16 shows the mean bed level changes, analyzed within the area of the formerly channelized riverbed, between the state in 2001 and 2019. The bed level changes show the adjustment of the channel slope to re-establish the sediment transport capacity in the widened bed.

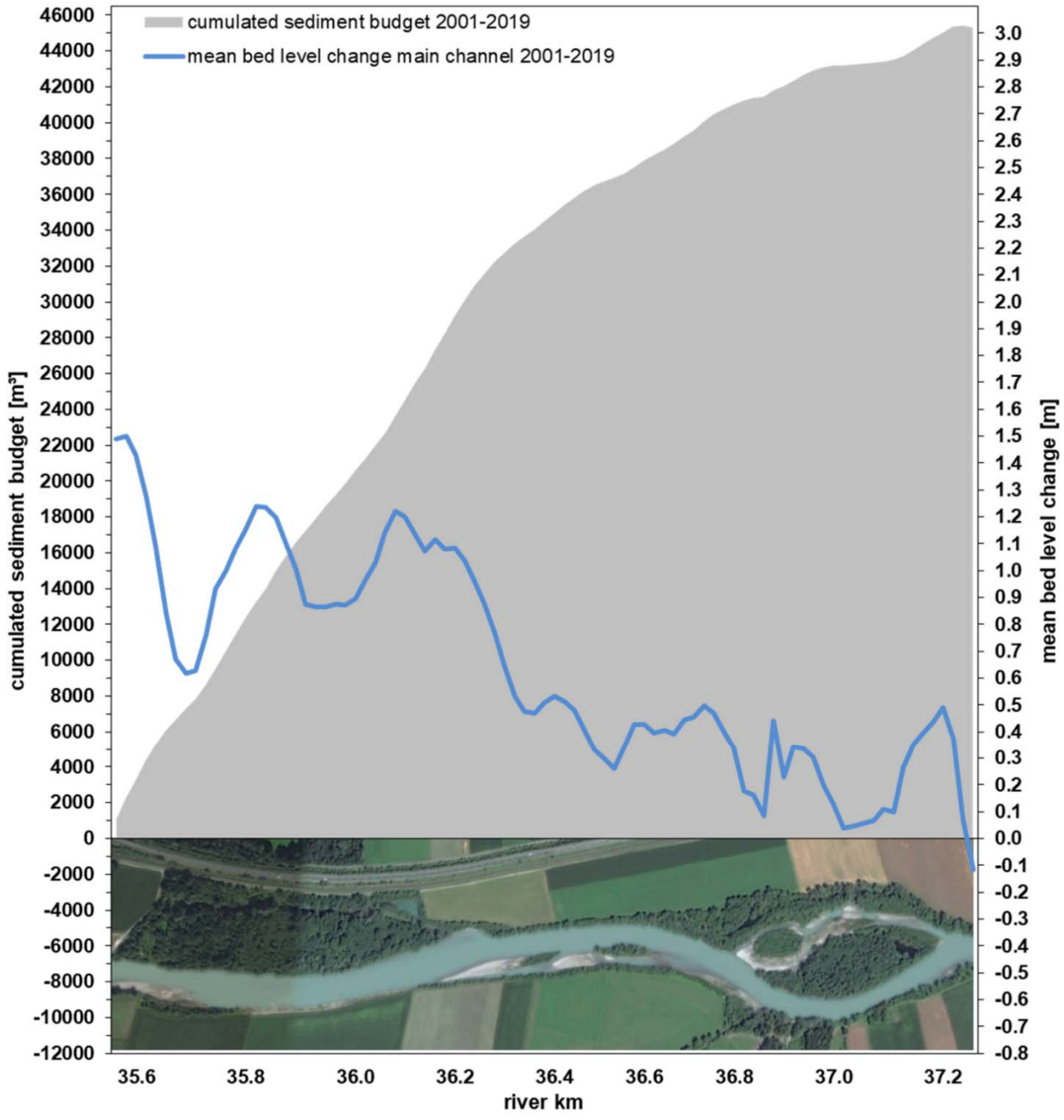

Figure 16 Cumulated sediment budget and mean bed level change in the period between 2001 and 2019.

Figure 17 shows the mean bed elevations for all elevation models compared to the initial bed elevation before measure implementation. All values were derived within the widened area of 2003 in the main channel. Between km 36.2 and km 36.8 the bed levels

seem to have reached an equilibrium condition already before the flood event in October 2018. The main channel section, which is located next to the side-channel, showed aggradation which exceeded 0.5 m in the year 2003, but nearly changed back to the initial condition when the side-channel became increasingly disconnected. Between km 36.2 and km 35.8 the bed was already widened in 2003 and bed levels reached an equilibrium state few years after measure implementation. In the widening, which was implemented in the year 2014 (km 35.8 to 36.1), the flood event of October 2018 still caused large aggradation, possibly not having reached an equilibrium yet. The widened section between km 35.6 and km 35.8 found a state close to equilibrium in 2011, but aggraded when the section downstream aggraded, probably to adjust the slope to re-establish sediment transport capacity in the widened bed.

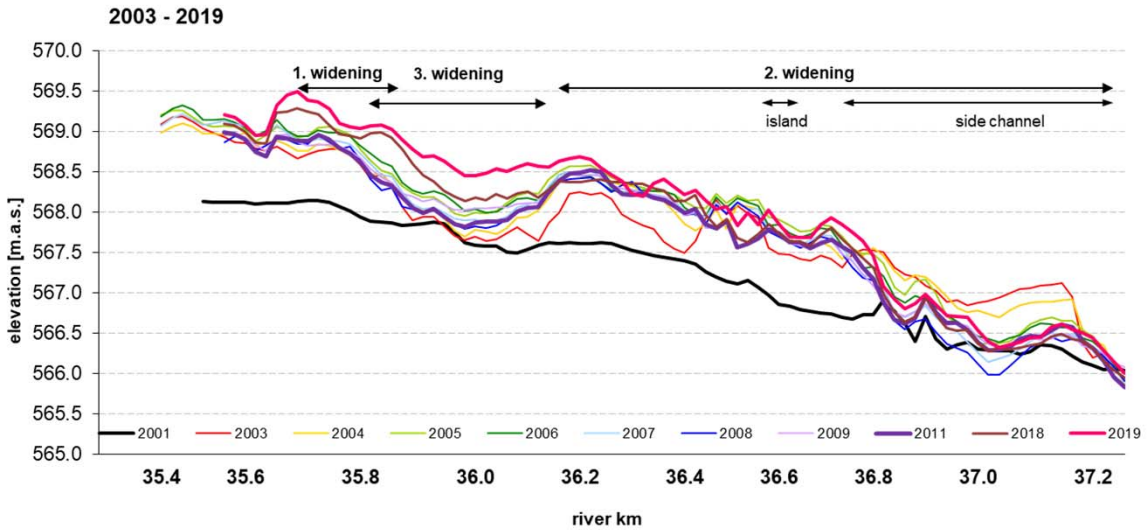

Figure 17. Mean riverbed elevations in the main channel, analysed in the area of the widened riverbed of 2003.

While the widening of the reach has an overall positive effect on the mean bed elevation, there is still incision at the confluence of both channels at km 37.3. The bed scour there may have resulted from the confluence situation itself, but it also may be the consequence of the sediment deficit given the large sediment consumption of the measure.

In addition to the sediment budget and bed level analysis, the method of Vázquez-Tarrío et al was applied to the Drau case study site to determine the bed surface sediment size from UAV imagery. Wolman Pebble counts served to determine the grain sizes distributions (Figure 18), which were used to calculate characteristic grain sizes.

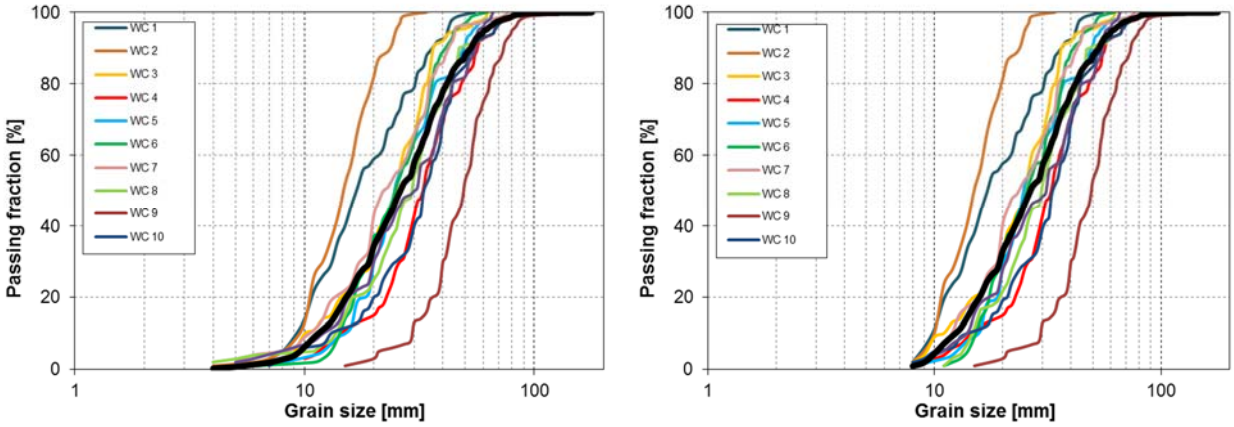

Figure 18. Grain size distributions of the Wolman Pebble Counts in the side channel auf the site at Kleblach-Lind. The diagram at the right shows a truncation of the grain size analysis at to improve later regression results following suggestions from Vázquez-Tarrío et al. (2017).

The DEM derived from UAV photogrammetry was used to calculate a surface roughness. Characteristic grain sizes were then related to statistical roughness parameters to find relations (Figure 19), which allow deriving the grain size from UAV photogrammetry.

The best relation was found by relating the d_{50} to the roughness height with a Kernel-radius of 0.5m. The results could be improved by removing one grain size sample which produced outliers in the relations and by truncating the grain size analyses at 8mm as shown in Figure 18. Figure 19 shows the derived relations.

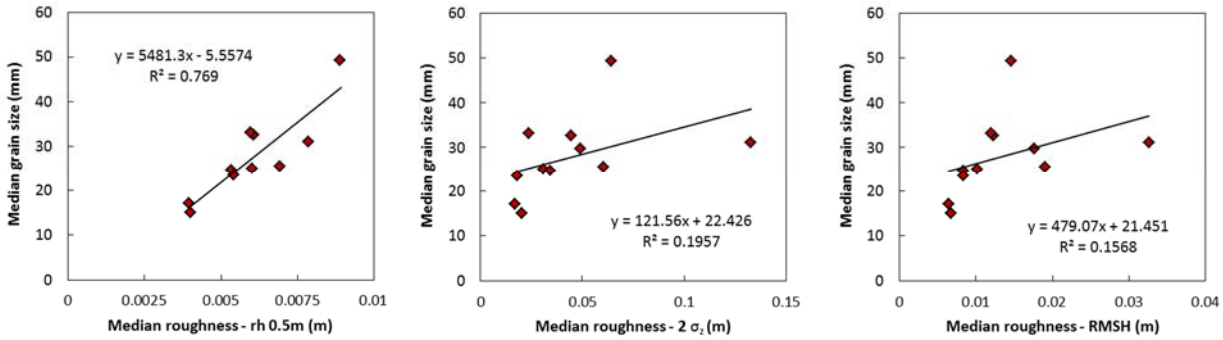

Figure 19. Rating curves between median values and median roughness values. The roughness height r_h delivered the best result.

The method based on the roughness height produced the largest coefficient of determination (r^2 = 0.769). This relation was then used to derive the grain sizes for the part of the side-channel, where the method was applicable (unvegetated and coarse-grained) (Figure 20) and also served to calculate changes (Figure 21).

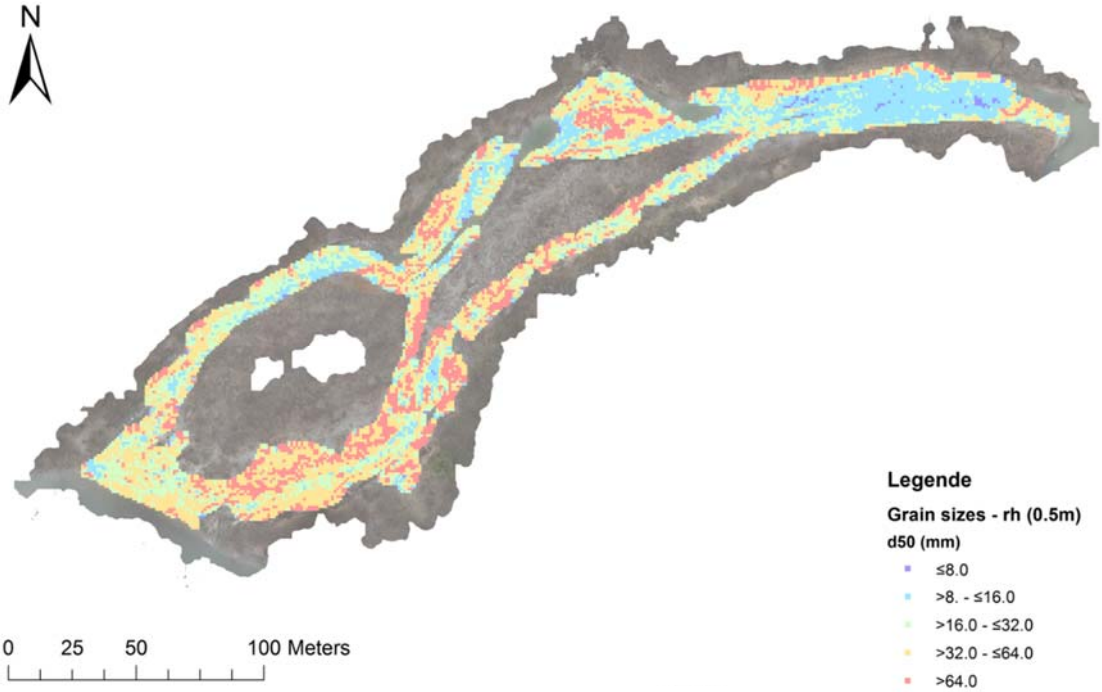

Figure 20. Surface grain size distribution derived from the UAV flight in April 2018.

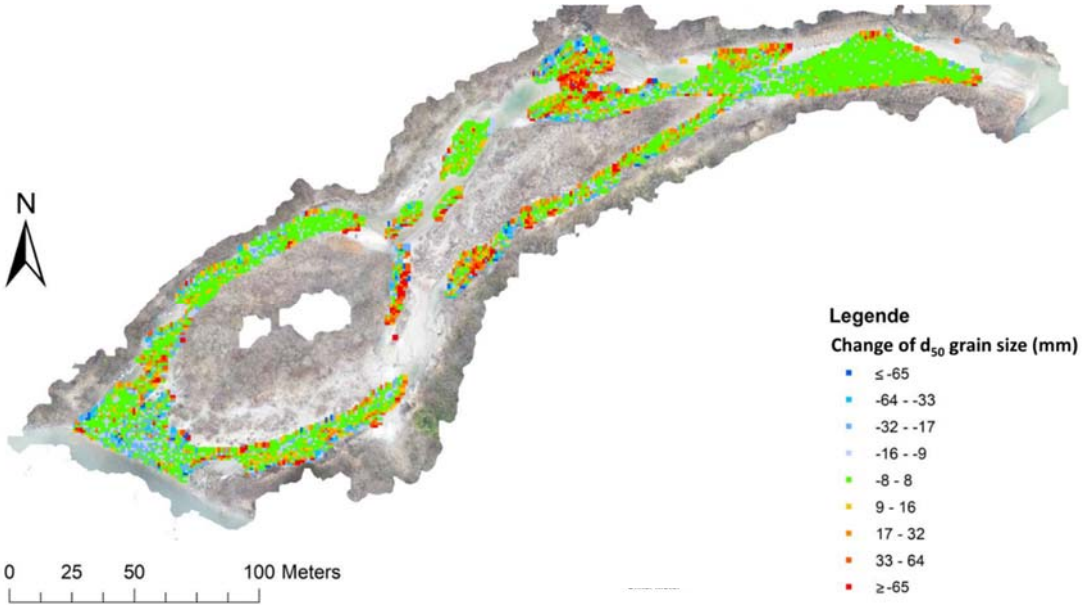

Figure 21. Changes in grain size between 2017 and 2018 based on the photogrammetric analyses of surface roughness and application of a formula relating grain size to surface roughness values.

3.1.2 Sediment transfer in the Upper Drava valley

After the tracer stones were inserted into the Drau River on May 11th, 2017 their positions were located eight times (Figure 22) between May 18th, 2017 and August 31st, 2017. The tracers were transported unexpectedly fast so that at the last analysed survey half of the tracers already crossed the antenna cross section, which was intended to mark the downstream end of the surveyed section (5 km downstream of the insertion location). However, the tracers could be easily detected from large distances (> 50m) and given the great support from the local water management authority in providing a boat and the high motivation of their staff member, the tracking distance was extended to whatever length needed. The survey period included two flow events with discharges around a one-year flood (Figure 22).

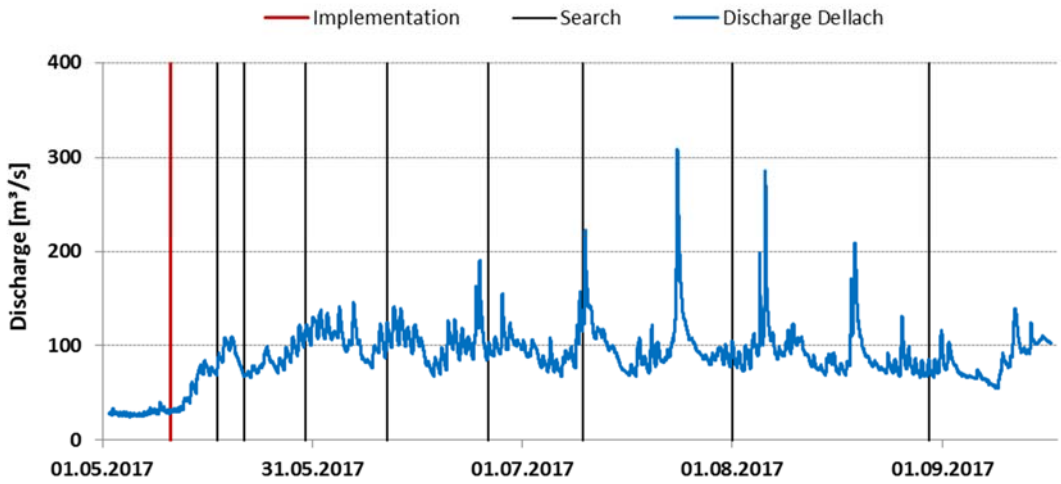

Figure 22. Dates of tracer insertion and of the repeated surveys in relation to the discharge time series.

Figure 23 displays the tracer positions in the Upper Drau valley at the first the first (May 18th, 2017) and last analysed survey (August 31st, 2017). Two surveys in 2018 revealed that some tracers already ran out of battery so that these surveys were not included in the analysis. A tracer of the second-smallest size class (b-axis=38.1mm) reached the longest travel distance and was located in the side-channel of the widening near the village of Obergottesfeld, in close proximity to the mid-channel bar section analysed in chapter 3.1.3.

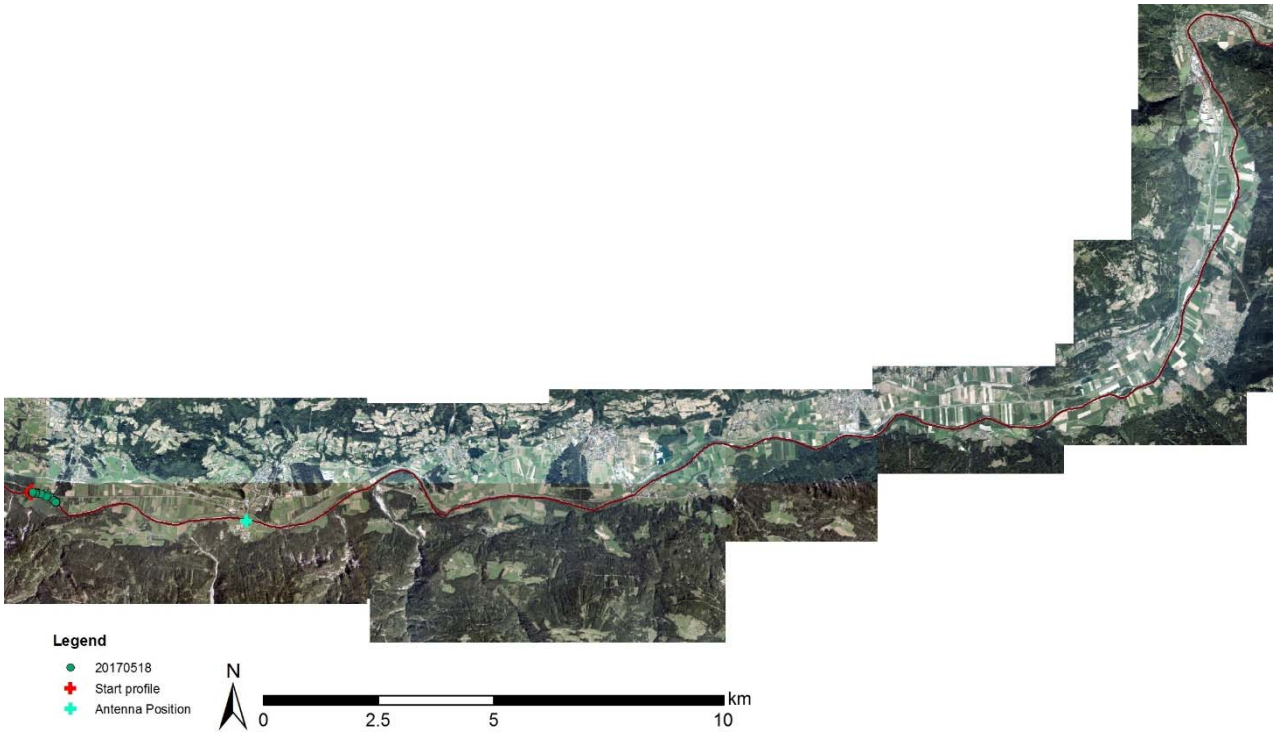

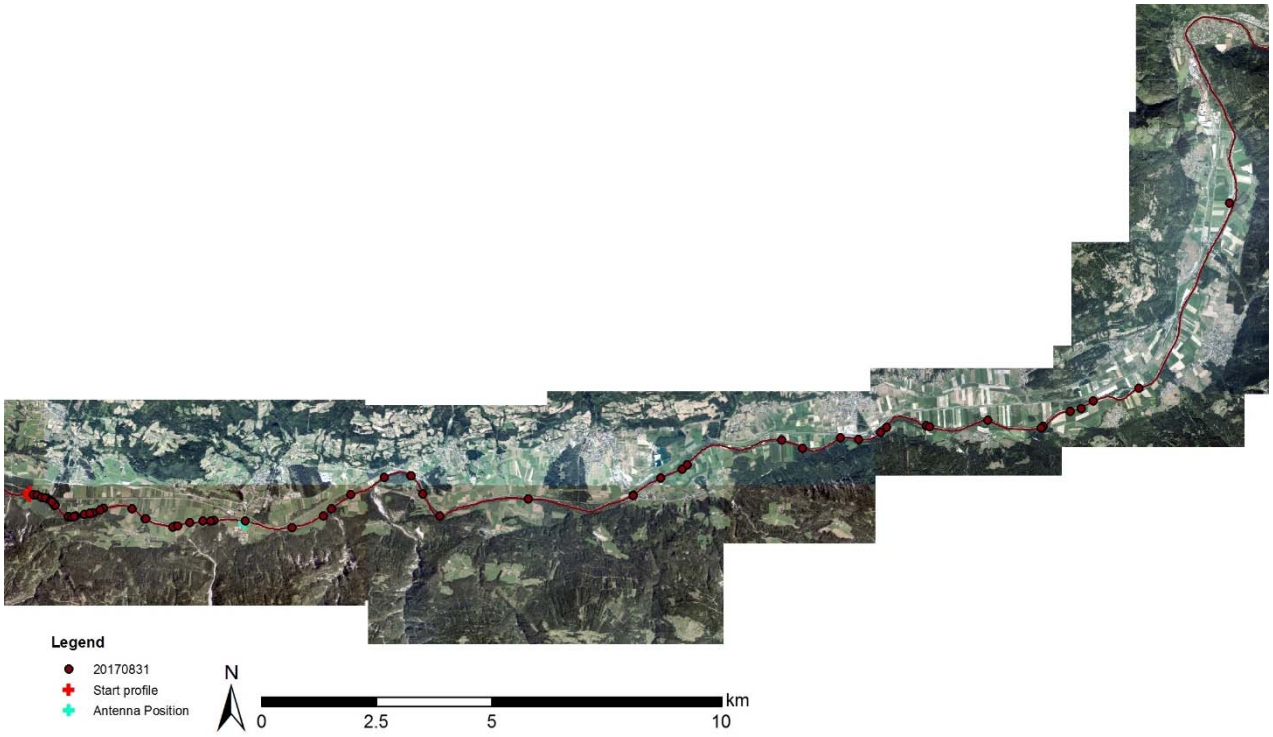

Figure 23. Tracer positions at the first (May 18th, 2017) and last analysed survey (August 31st, 2017). Two surveys in 2018 revealed that some tracers already ran out of battery so that these surveys were not included in the analysis.

Figure 24 shows the distribution of the different size classes on August 31st, 2017. The travel distances show a clear dependency on the grain size of the transported grain.

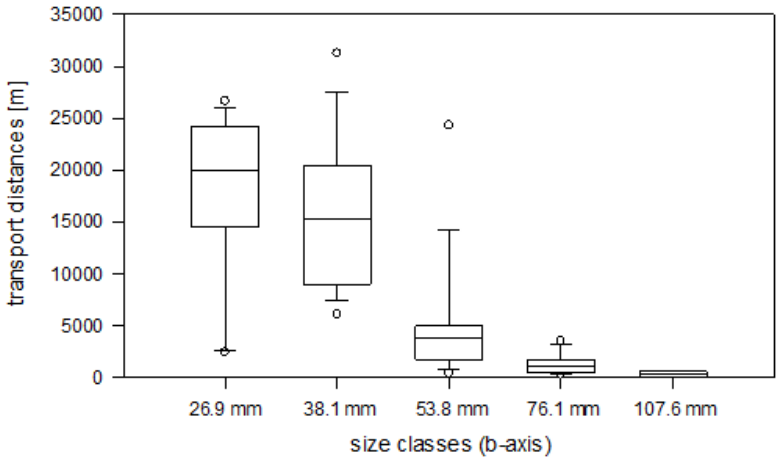

Figure 24. Box plots displaying the distribution of the tracers on August 31st, 2017.

All data was then used to derive a formula for the transport velocity of bedload. The regression method developed by Klösch and Habersack (2018) was further developed in HyMoCARES to account for the slowdown processes which result from effects such as burial and replacement of the tracked tracer stone by a natural stone. By eliminating slowdown effects, the unsteady virtual velocity corresponds to the bedload velocity at the actual shear stress (averaging hops and rest periods) and is calculated via:

$$V_u = 0.21e^{3.63\left(\frac{d}{d_{50}}\right)}\sqrt{\frac{\rho_s-\rho}{\rho}gd}\left[\frac{\tau}{(\rho_s-\rho)gd}-0.021\left(\frac{d}{d_{50}}\right)^{-0.485}\right]^{\frac{3}{2}}$$

where V_u (m s^{-1}) is the unsteady virtual velocity, d (m) is the length of the b-axis of the grain size of interest, d_{50} (m) is the median grain size of the sediment at the bed surface, ρ_s (kg m^{-3}) = the density of the sediment, ρ (kg m^{-3}) = the density of water, g (m s^{-2}) is the gravitational acceleration and τ = the bed shear stress (N m^{-2}).

The formula was implemented in the tool SedRace (D.T2.3.1), which allows practitioners to apply the formula to their own site.

3.1.3 Processes leading to excessive widening in the widening near Obergottesfeld

The time-lapse cameras were installed during the peak of the flood event on October 30th, 2018. The concave shape of the observed bank section protected the bank from erosive flow during the flood event. It was not before the 16th of December when the first riverbank failure was recorded by the time-lapse cameras. Figure 25 shows the hydrograph of the flood event, which reached a discharge of 600 m^3s^{-1}, and the low flow period which followed.

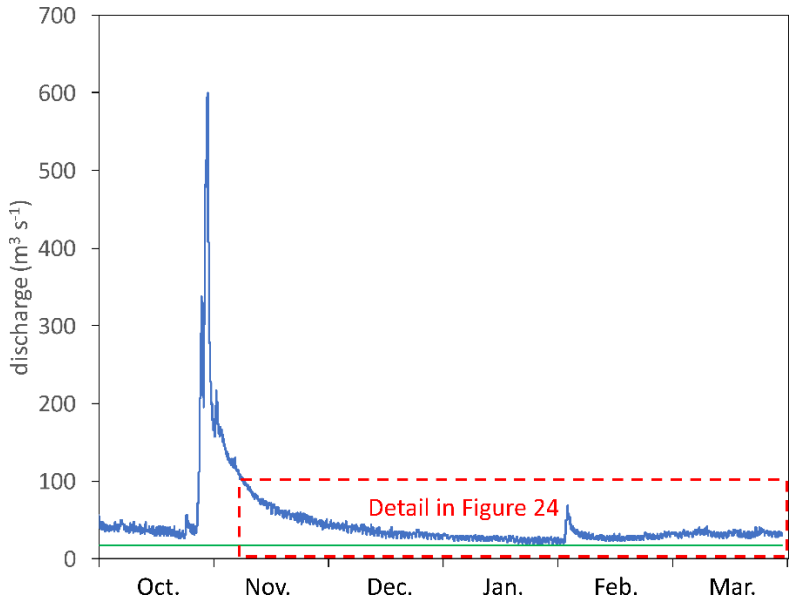

Figure 25. Discharge time series at the gauging station Sachsenburg during the flood of October 30th, 2018, and during the following low flow period during winter.

Figure 26 shows the falling limb of the flood hydrograph and the following low flow period, with marked bank erosion timings. Interestingly, even then bank erosion seemed to only occur when the discharge fell to an unprecedented small value.

To capture this morphodynamic processes, the riverbank and the mid-channel bar were subsequently surveyed using a total station, terrestrial photogrammetry and UAV to derive DEMs. Figure 27 shows the DEMs which were derived from a survey in December 2018 and another survey in March 2019.

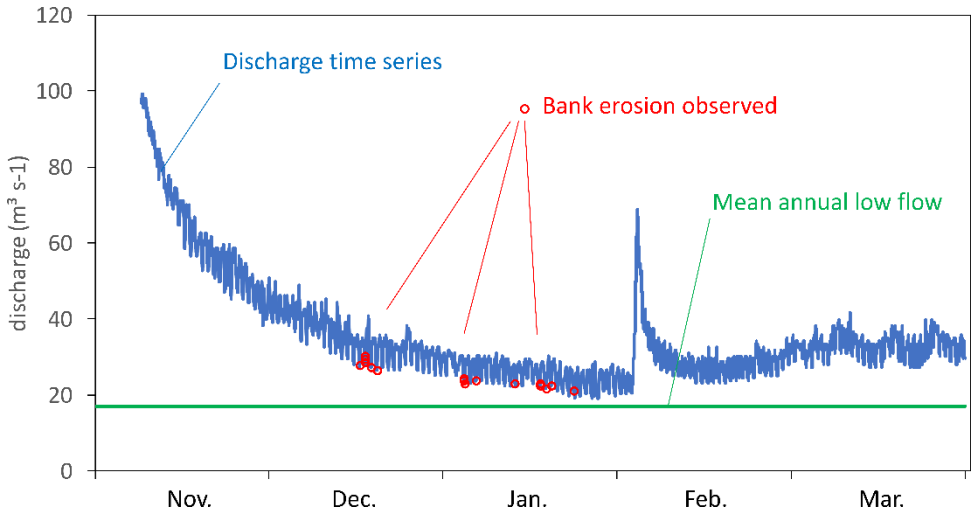

Figure 26. Falling limb of the flood event, low flow period, and small event interrupting the low flow in February. Red circles mark the timings of recorded bank erosion.

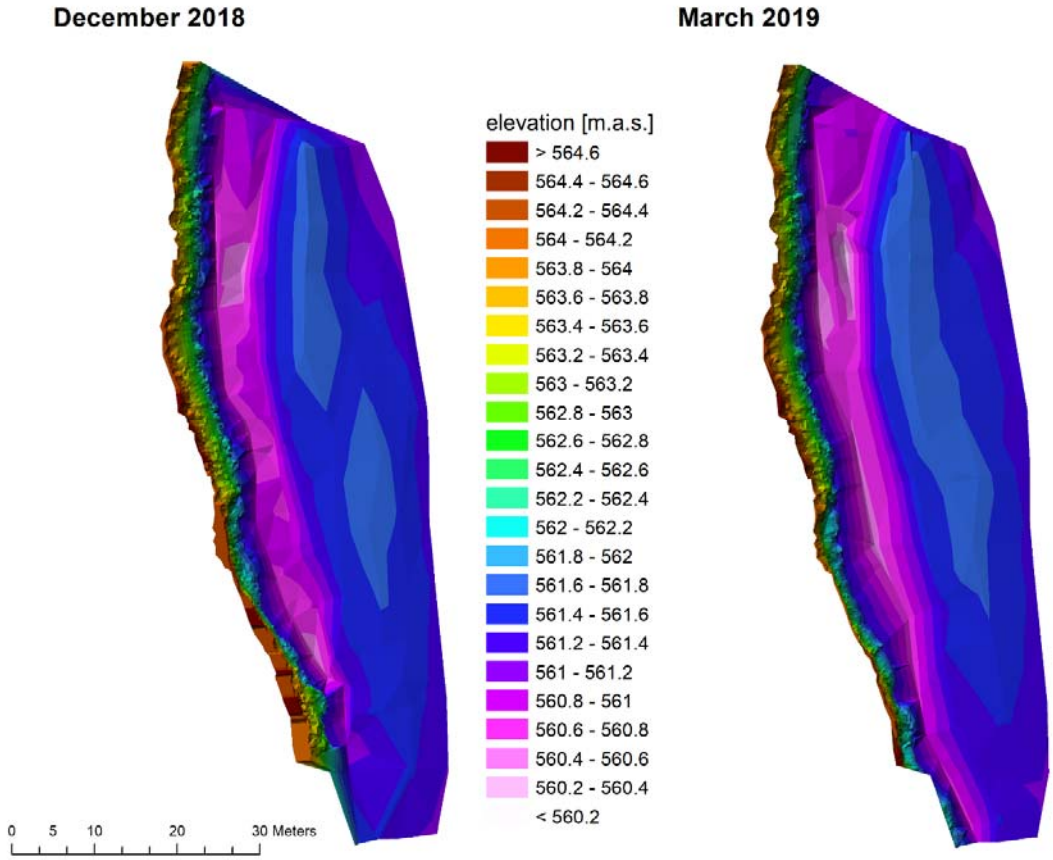

Figure 27. Left riverbank with gravel bar in December 2018 (left) and in March 2019 (right)

Figure 28 shows the elevation differences which resulted from the morphodynamics during the low flow period. The upstream part of the bank was massively eroded. The time-lapse images revealed that the bank erosion started upstream and propagated downstream as the discharge decreased.

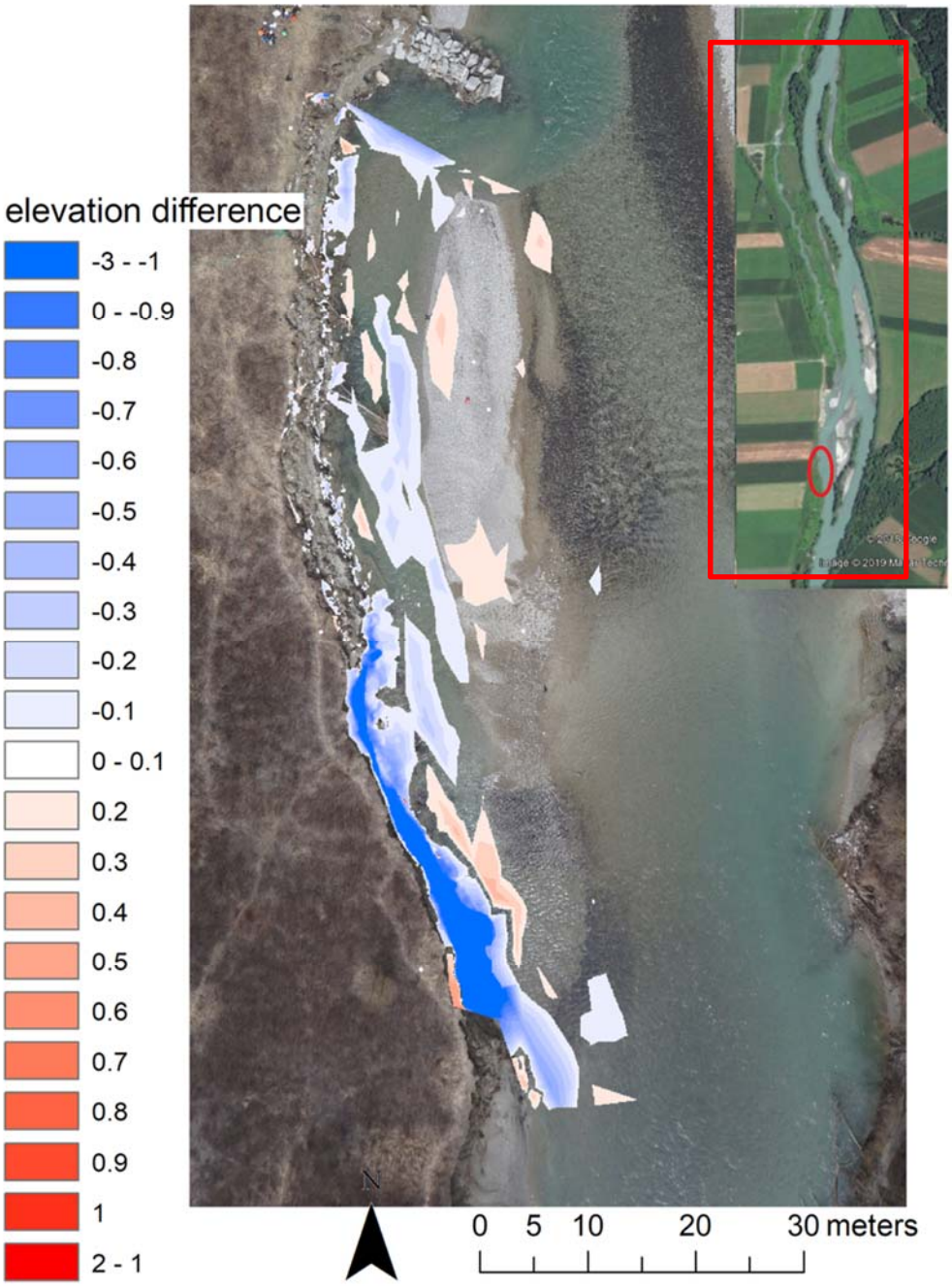

Figure 28. DEM of difference for the period between October 2018 and March 2019.

The observations confirmed the sequence of processes, which were described by Klösch et al. (2015) in a conceptual model (Figure 29):

1 The flow is diverted at lower discharges by the mid-channel bar. Bank profiles are steep, flow velocities and shear stresses below critical values.
2 During a flow event, the maximum flow velocities shift away from the riverbank. bedload transported from upstream is deposited on both sites of the bar head. The bar is fully submerged.
3 Returning to a low level, the flow is again diverted by the mid-channel bar. Due to the newly developed bar geometry, the thalweg is shifted towards the bank. Sediment deposition increased the elevation of the riffle, leading to an increased energy slope downstream. In combination, this results in flow velocities and shear stresses exceeding critical values for bed and bank erosion, leading to undercutting of the bank, resulting in sliding and/or toppling of failure blocks.
4 The channel has completely adjusted to the bar accretion and is capable of carrying a range of discharges while remaining stable until the next flow event.

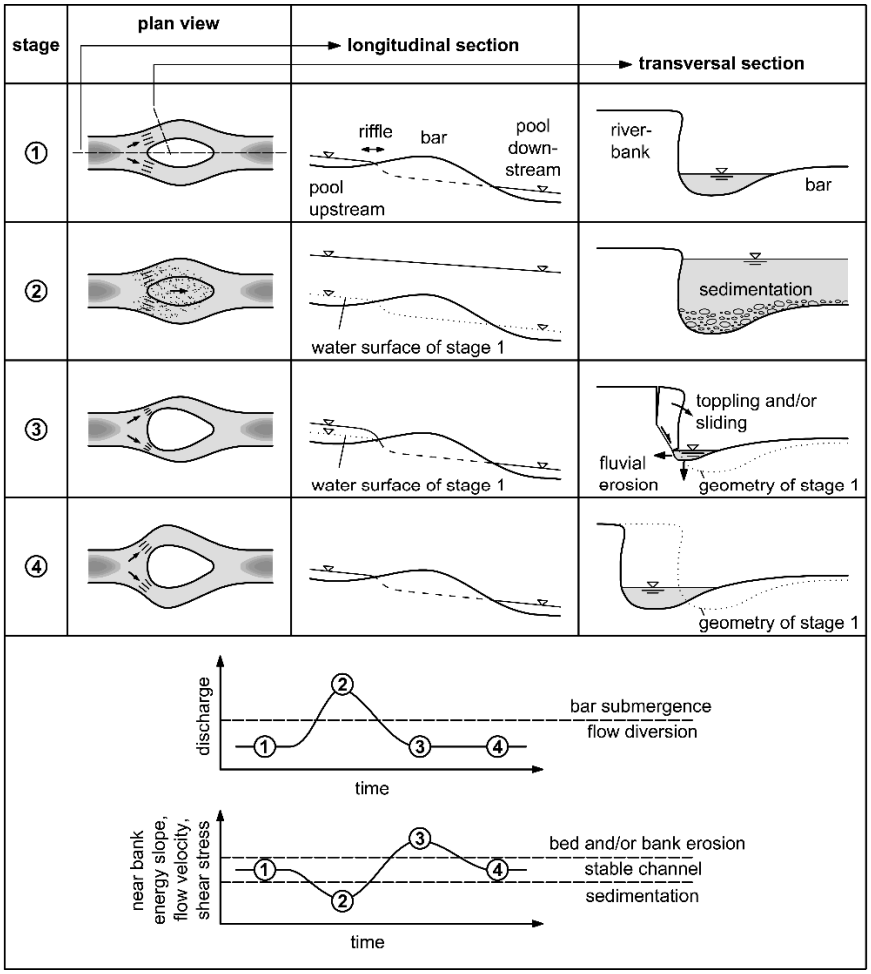

Figure 29. Interactions between mid-channel bar growth and bank erosion (Klösch et. al., 2015)

Due to the interruption of the low flow period, the process as described by Klösch et al. (2015) could only take full effect in the upper third of the surveyed area, resulting in an embayment with steep riverbanks (Figure 28; blue area). A further decrease of the discharge in the winter would have led to a progression of the erosion further downstream. However, the small flow event in February interrupted the low flow period and the processes stopped. Additionally, rip-rap blocks which were installed in the hinterland became already exposed 30m downstream of the freshly eroded embayment, and would have probably stopped the downstream progression.

Two cameras were installed to increase the chances for success of obtaining a continuous record of the bank section. As the cameras were mounted in approximately 1m distance, both directed towards the bank and mid-channel bar section, their potential for photogrammetric analysis could be tested (Figure 30). As the processes

occurred in too large distance to the cameras, this potential could not be used here. However, it was identified as a potentially useful method in the monitoring of restoration measures.

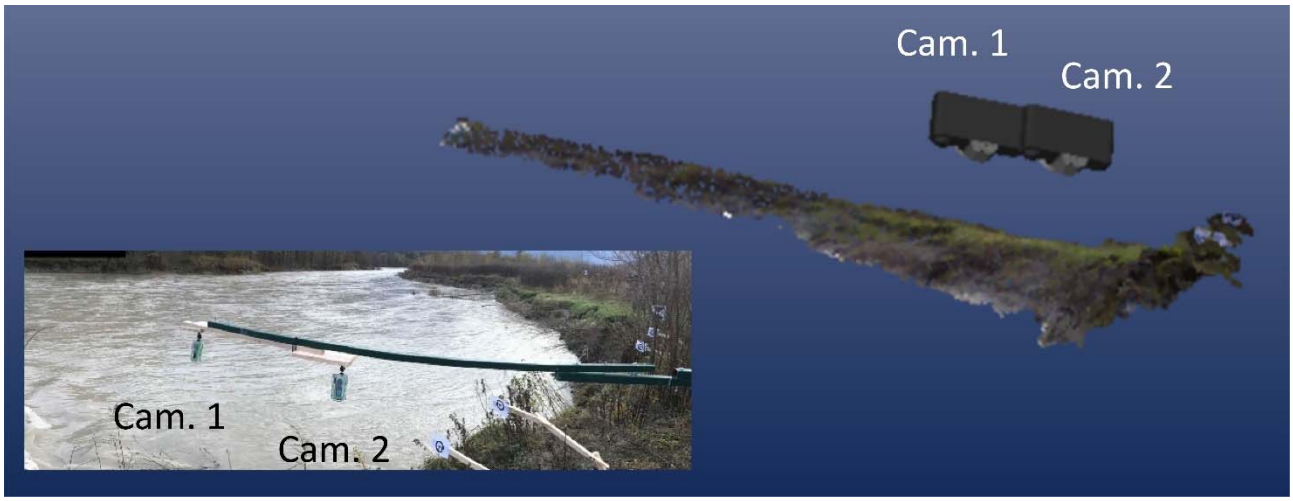

Figure 30. Test of using two time-lapse cameras for continuous monitoring of riverbank geometry.

3.2 Mur River

Riverbank erosion

In the course of the Dra-Mur-CI Project, a repeated terrestrial photogrammetry was used to measure the progress of riverbank erosion. In 2012, a maximum of 12 m was surveyed at the location of P1 (displayed in Figure 31). A regression analysis, which considered the discharge time series and repeated bank retreat measurements, delivered a formula describing the bank retreat as a function of discharge. Based on a 60-years hydrograph, the formula yielded an average erosion rate of 2.07 m/year for the bank upstream of the inlet of the Saßbach. The 60-years hydrograph was artificially created and used in the Basic Water Management Concept as a forecast hydrograph for the deployed sediment transport model (Austrian-Slovenian Standing Committee for the Mur River, 2001). By using the long hydrograph, the bank retreat formula provided an average value which is independent from the few flow events which occurred in the investigation period.

Figure 31. a) Mur river case study site near Gosdorf with surveyed cross-sections, b) left bank of cross-section P1, c) left bank of cross-section P2.

HyMoCARES now allowed a resurvey of the riverbanks. Figure 32 shows the bank surface in 2018 compared to the cross-sectional geometry after measure implementation in 2007.

The survey revealed a maximum bank retreat downstream of an outcrop of tertiary rock sediment, which directed increased flow velocities towards the bank. There a bank retreat of 22 m was measured, which corresponds to an average retreat rate of 1 m/year. Cross section 1 in Figure 32 represents the location of this maximum. While this clearly shows the initiation of bank erosion, the bank retreat did not match the expected extent. In cross section 2 (Figure 32), a section with uniform geometry and not hydraulically disturbed by the upstream tertiary outcrop, the bank retreat only reached 5m.

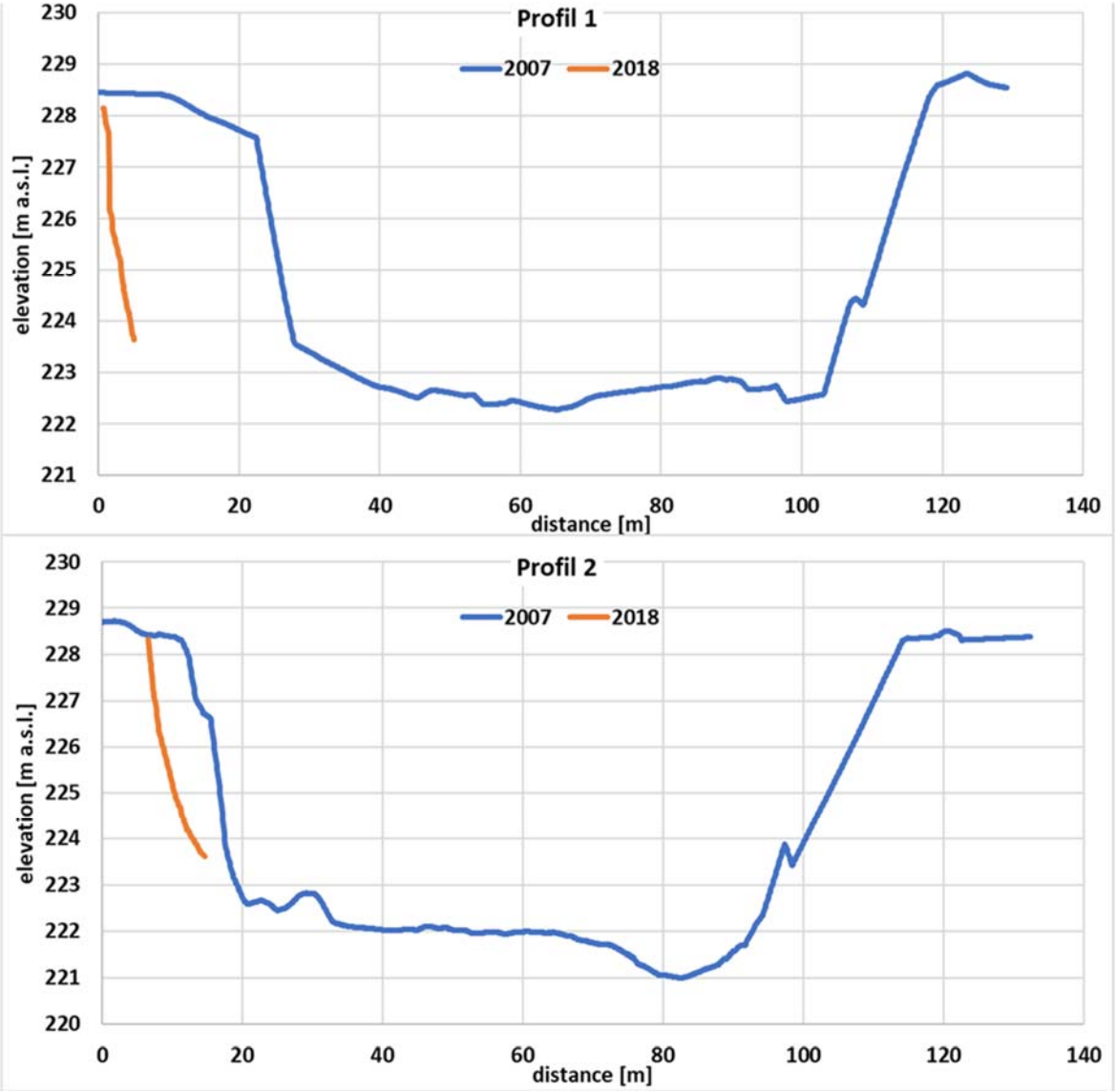

Figure 32. Cross-section geometries after completion of measure implementation in 2007 and in 2018 after self-dynamic widening.

Bed level changes

The development of the bed elevation was monitored from 2007 to 2009. During this period, a positive effect of the widening was assessed in the restored reach as well as in the constrained section 10 km further downstream of the restoration site. A part of the sediment deposited in the widened section was still available for bed stabilisation as well as for dotation of the confined reach, where the bed level was raised by 0.24m.

(Dra-Mur-Ci, 2013). Considering the slow bank erosion rates and the small delivery of bank-derived gravel further analyses of the bed levels are urgently needed.

Erodibility of tertiary sediments

During a period of low flow in August 2019, the Mur site was visited to analyse the condition of the riverbed and the erodibility of the tertiary sediment. Tertiary outcrops were visible at several places of the riverbed. The tertiary sediment, which was detected, did not consist of loose fine grains such as sand or silt, but was compacted, appearing like sandstones. On a plane bar downstream of the large outcrop which crosses the entire river, several deposits of transported tertiary sediment could be detected (Figure 33).

Figure 33. Deposits of transported tertiary sediment on a bar downstream of a large tertiary outcrop. A Fifty Euro Cent coin is used as a scale.

The deposits were rounded as pebbles, but mostly showed high fragility. It is unclear whether these tertiary particles were mobilised during maintenance works with an excavator which occurred in the same year, or whether these particles were mobilised due to fluvial action. Tertiary outcrops were visible at this low flow condition at several locations (Figure 34a) and submerged outcrops were visible at the water surface (Figure 34b).

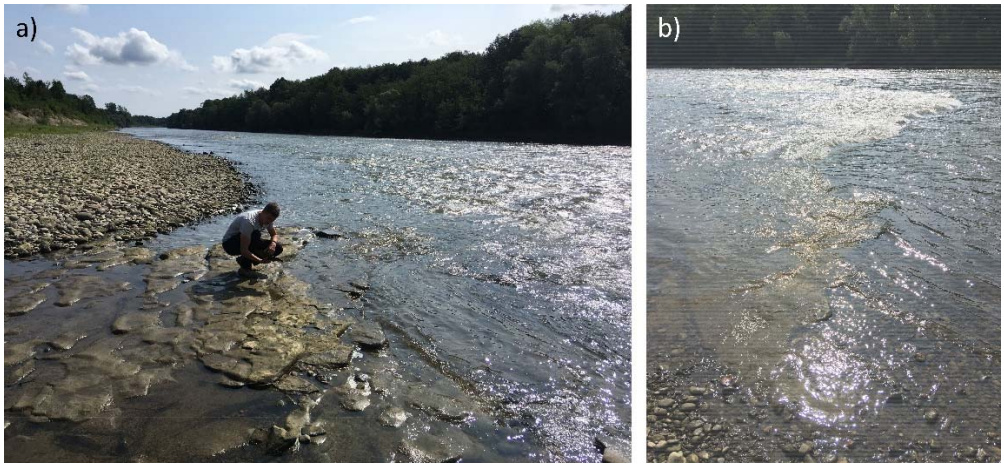

Figure 34. a) Tertiary outcrop and b) hydraulic effect of a tertiary outcrop.

The tertiary sediment outcrops, which were accessible, could easily be broken into plates using a cramp (Figure 35a), given interbedded layers of more loose, fine sediment. Both, the deposited tertiary pebbles and the outcrops could easily be scratched with the thumbnail (Figure 35b), suggesting a little resistance to abrasion.

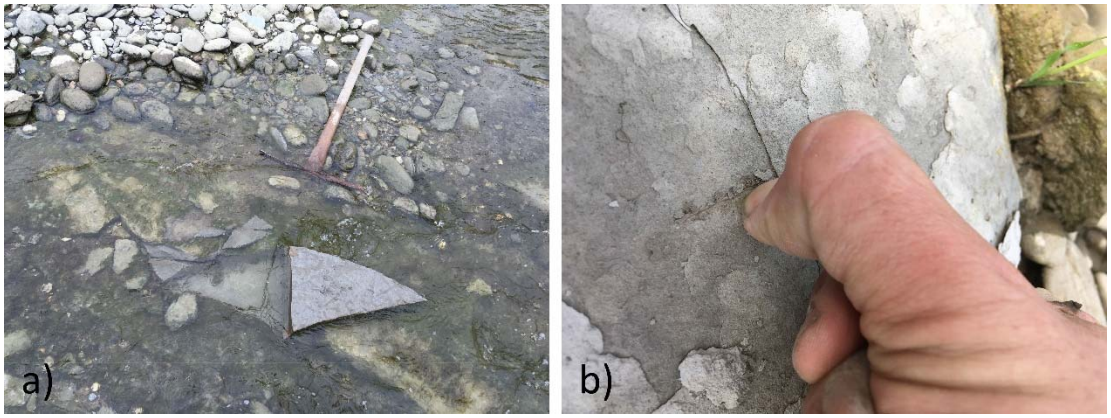

Figure 35. a) Tertiary sediment which can be loosened as plates, b) tertiary sediment can easily be scratched with a thumbnail.

The jet test allowed testing the resistance to fluvial erosion. By installing the head tank on top of the riverbank, a shear stress of 130 N m^2 could be applied onto the surface of the tertiary sediment. Despite the high shear stress the jet did not scour the sediment, so that the critical shear stress must be higher than this value. As no scouring occurred, the erodibility coefficient could not be determined. The high critical shear stress (>130 N m^{-2}) indicates, that the tertiary material is not eroded by fluvial erosion. However, it needs to be considered that only a very limited part of the tertiary sediment was accessible and that the accessible material may be of higher resistance than other

tertiary sediment. If the tertiary sediment is not fluvially eroded, the abrasion due to bedload transport on the tertiary sediment may still be an issue. The development of biofilms on immobile tertiary sediment may protect the sediment also from abrasion.

Moreover, it has to be considered that the tertiary material's appearance as plates with interbedded layers of loose, fine sediment suggests an anisotropy of the materials properties. The jet was applied perpendicular to the surface of the plates. If the Jet would be placed parallel to the material's layers, a higher erodibility can be expected. This alternative setup could not be realised, as the sides of the plates were smaller than the instrument, and given the fact that the method of analysing jet tests assumes isotropy of the material. However, the effect of anisotropy may be important as the erosion of more erodible layers may loosen entire plates of the tertiary material, which then may disaggregate and abrade during transport, a process different from fluvial erosion.

3.3 Salzach River

The tool "Chevo", which was developed in HyMoCARES, was applied to the 800 m long section of the Salzach downstream of the step-pool-ramp, with the purpose to use a standardized assessment of the bed evolution. From this section, cross section data was available from before (2005) and after (2015) measure implementation (Figure 36).

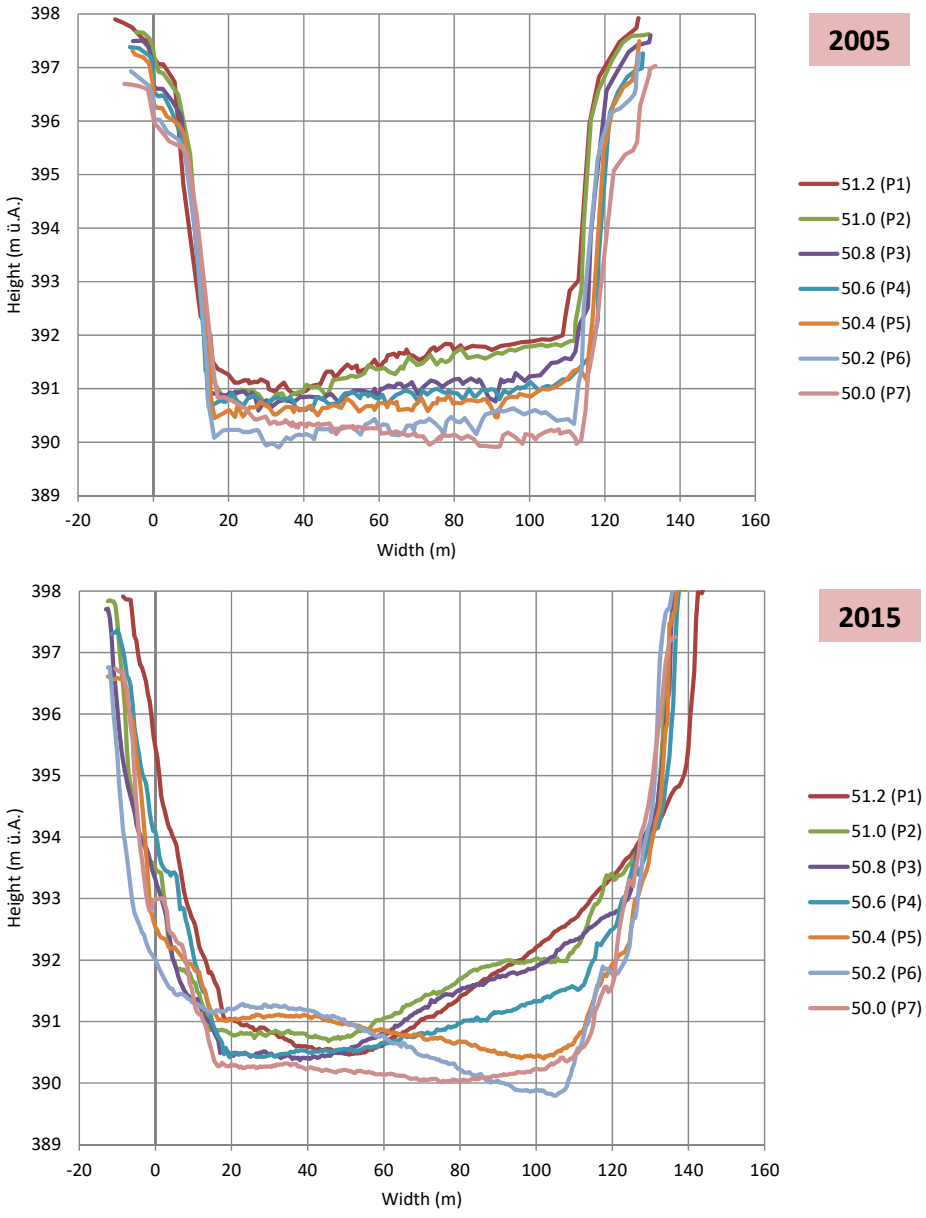

Figure 36 Bed level measurements downstream of the step-pool-ramp before (2005) and 5 years after the erection of the ramp (2015).

Chevo recommends the use of the effective discharge for analysing the mean bed levels of the wetted perimeter, as the effective discharge transports the most sediment and is recognised as the 'channel-forming' discharge. At the Salzach, the mean annual discharge was assumed to be similar to the effective discharge, and was modelled with Chevo in the seven available cross sections between km 51.2 (P1) and 50.0 (P7). Figure 36 exhibits a channel widening for the mean annual flood as the main morphological change.

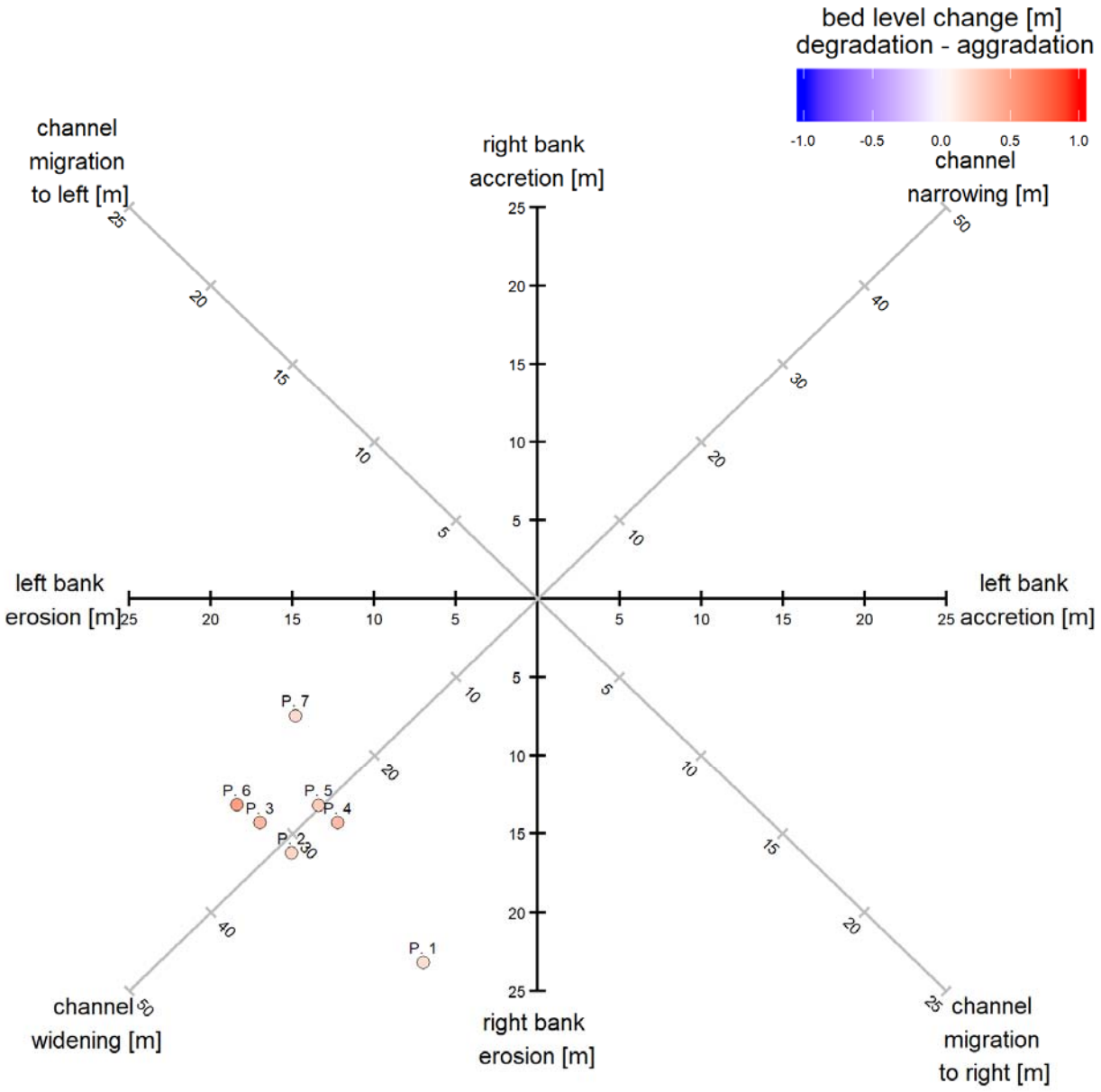

Figure 37. Results of applying Chevo to a section of the river Salzach between km 51.2 (P1) and 50.0 (P7) for low discharge (NQ)

All cross sections showed an aggradational trend, indicating that the bank retreat successfully compensated the sediment deficit which resulted from the construction of the step-pool ramp. Additionally, the analysis was performed for a low flow discharge. For a low discharge, Chevo points out the accretion of the right bar as the main morphological change and shows a degradation within the perimeter (Figure 38).

The monitoring of the bed levels should be continued to eventually react in time with counter measures.

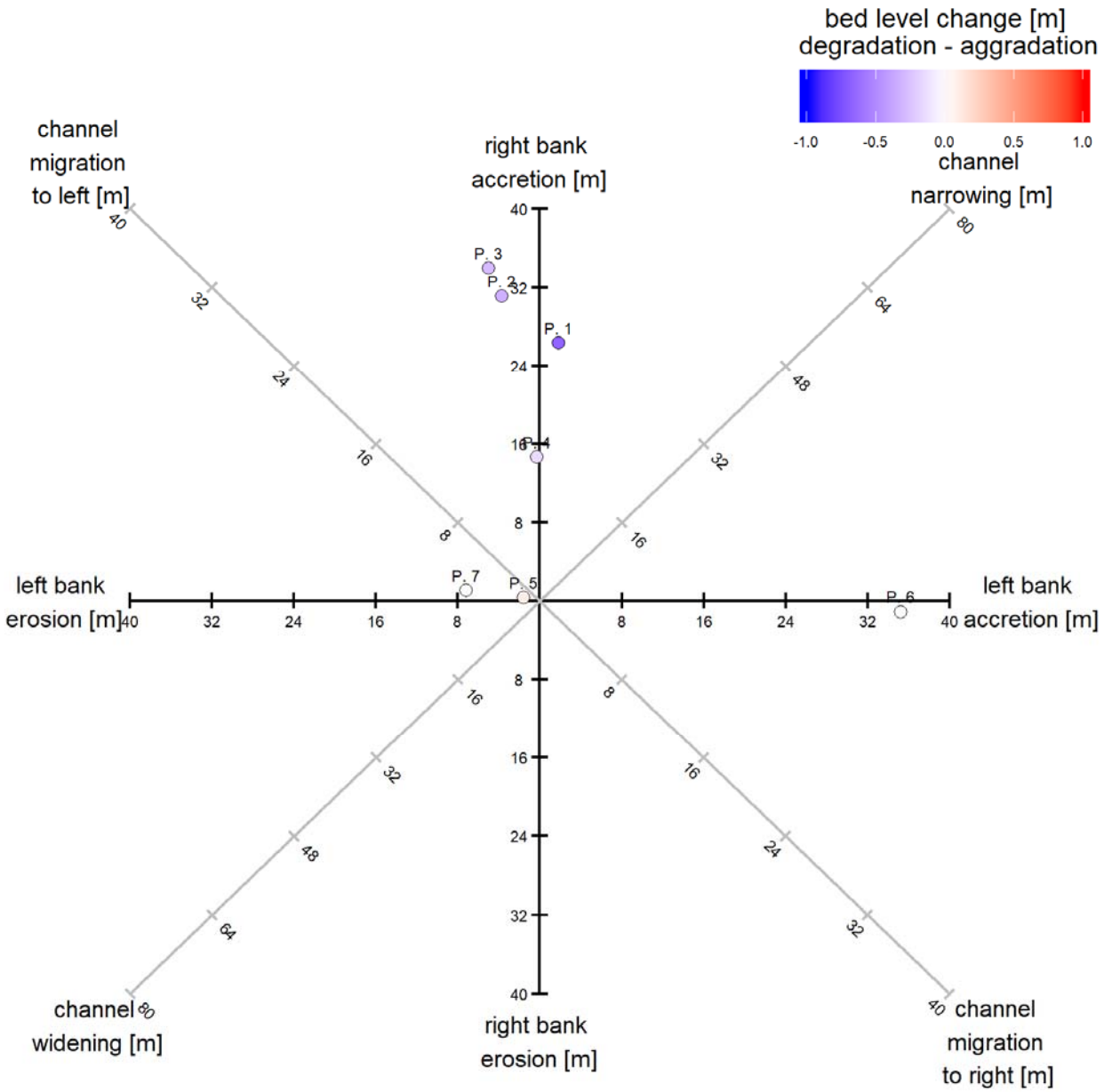

Figure 38 Results of applying Chevo to a section of the river Salzach between km 51.2 (P1) and 50.0 (P7) for the mean annual flood (MJHQ)

4 Ecological effects

4.1 Drau case study

A three-year post-treatment monitoring compared the ecological status of channelized reaches with restored reaches and the deviation of the treatments and controls to type-specific reference conditions.
The monitoring results showed an increase in habitat variety like stagnant shallow zones, riffle areas, gravel and sand bars, which are essential habitats for gravel spawners. Fish sampling showed an increase in the key species European grayling (Thymallus thymallus), while the Brown (Salmo trutta) and rainbow trout (Oncorhynchus mykiss) showed little difference between restored and control reaches. (Roni et al., 2013)
Overall, the situation for fish fauna, especially for juvenile fishes, has improved. Newly created gravel bars and shallow water zones are accepted as habitat by a variety of bird species, e.g. the little ringed plover (Charadrius dubius), the common sandpiper (Actitis hypoleucos) and the kingfisher (Alcedinidae). Concerning amphibians, the number of potential spawning habitats has doubled, which led to the introduction of two new species (Hyla and pool frog) and to an increase in the population of yellow-bellied toads. As this survey was made in 2003, shortly after finishing the restoration work, it will take a few years for the full effects of these measures on amphibians and avian fauna to be visible. (LIFE Project, Auenverbund Obere Drau Endbericht, 2003)

4.2 Mur case study

The implemented measures tripled the length of the bank line, compared to the initial state, indicating an improved habitat diversity. The steep natural banks, gravel bars, and fine sediments were recolonized by endangered bird and insect species (H. Brunner et al., Zoologisches Post-Monitoring in Aufweitungen der steirischen Grenzmur, report for the Styrian water management and nature protection authorities, unpublished, 2010)

5 Conclusions and perspectives

5.1 Sediment consumption and need of bed widenings

Despite many impacts, the Drau River still possesses considerable sediment supply. A long-term monitoring at the Drau River showed lateral dynamics, development of a more natural morphology, and the related sediment consumption of a river widening measure. At the Mur River, sediment supply was negligible and lateral dynamics and development of a more natural morphology remained below expectations.

It shows that enough sediment supply should be provided to allow a more natural morphology to develop, because

- The morphology depends on sediment supply (see Multiscale diagram in deliverable D.T2.2.1)
  The more natural morphology consumes sediment until it is fully developed and continuity is re-established because of a higher river bed and aggradational features.

5.2 The role of channel constraints for river morphology

At the Drau River, channel constraints in the restored reach fixed the position of the larger bars in place. After a 10-year-flood destroyed the inlet protection of the island which separated the side-channel from the main channel, the boundary conditions for the river morphology were changed. New dynamics occurred (bank erosion, aggradational features). A further widening which was implemented in 2014 within the original measure section of 2003 had a similar effect; in that case the change of boundary conditions re-initiated morphodynamics also in the downstream and upstream section. A large bar, which appeared to be stable, was eroded and made room for new aggradational features, which are very important in providing habitats for rejuvenation of riverine species (see the tool HyMoLink of the online HyMoCARES toolbox and deliverable D.T2.3.1).

The observation demonstrates that the channel constraints need to be limited to allow lateral dynamics over longer term. (The river freedom index, which was developed in HyMoCARES, may be used for evaluation of channel constraints, see deliverable D.T2.2.1)

5.3 The velocity of sediment transfer

The tracer study in the Upper Drau valley showed that sediment may be transferred rapidly if it occurs on an armoured riverbed in mostly channelized river sections. Sediment replenishment with the aim to counter bed degradation needs to be coupled with channel widening to decrease shear stresses, slow down bedload transport,

increase the residence time of the sediment in the target reaches and trigger sedimentation.

5.4 Riverbed breakthrough indicator

While the encountered Mur Tertiary sediment showed to be inerodible regarding fluvial forces (at least in the setup with a jet perpendicular to the material's layering), it showed a little degree of hardness (it could be scratched with the fingernail) and little stability (it easily breaks into pieces). The velocity of abrasion due to bedload transport on the material, and the effect of the material's anisotropy are unknown and are still to be examined.

5.5 Bar-bank interactions

Mid-channel bars, which appear in formerly wandering rivers after restoration, are accompanied with excessive widening. The largest bank retreat rates may occur during the lowest discharges following the flood event. Climate change, which may increase the discharges in the winter, may reduce the development of cutbanks which are then missing as habitats for e.g. bank-nesting birds.

6 References

Austrian-Slovenian Standing Committee for the Mur River (2001), Basic Water Management Concept–Phase I, report, Vienna.

Bunte, K., & Abt, S. R. (2001). Sampling surface and subsurface particle-size distributions in wadable gravel-and cobble-bed streams for analyses in sediment transport, hydraulics, and streambed monitoring. Gen. Tech. Rep. RMRS-GTR-74. Fort Collins, CO: US Department of Agriculture, Forest Service, Rocky Mountain Research Station. 428 p., 74.

Chapuis, M., Bright, C. J., Hufnagel, J., and MacVicar, B. (2014), Detection ranges and uncertainty of passive Radio Frequency Identification (RFID) transponders for sediment tracking in gravel rivers and coastal environments, *Earth Surf. Process. Landforms*, 39, 2109– 2120, doi: 10.1002/esp.3620

E. Formann, H.M. Habersack, Schober S. (2007). Morphodynamic river processes and techniques for assessment of channel evolution in Alpine gravel bed rivers, Geomorphology, 901 (2007), pp. 340-355, 10.1016/j.geomorph.2006.10.029

Klösch M., Blamauer B., Habersack H. 2015. Intra-event scale bar-bank interactions and their role in channel widening. Earth Surface Processes and Landforms 40, 15-06-1523 (2015), DOI: 10.1002/esp.3732

Klösch, M; Habersack, H The Hydromorphological Evaluation Tool (HYMET). GEOMORPHOLOGY. 2017; 291: 143-158.

Klösch M., Hornich R., Baumann N., Puchner G., Habersack H. (2011): Mitigating Channel Incision via Sediment Input and Self-Initiated Riverbank Erosion at the Mur River, Austria.

In: Bennett S. J., Castro J. M., Simon A., Stream Restoration in Dynamic Fluvial Systems: Scientific Approaches, Analyses, and Tools 194; American Geophysical Union; ISBN 978-0-87590-483-2

Roni P, Liermann M, Muhar S, Schmutz S. 2013. Monitoring and evaluation of restoration actions. In: Stream and Watershed Restoration: A Guide to Restoring Riverine Processes and Habitats, Roni P, Beechie T (eds). John Wiley and Sons: Chichester; 254-279.

Vázquez-Tarrío, D., Borgniet, L., Liébault, F. & Recking, A., 2017. Using UAS optical imagery and SfM photogrammetry to characterize the surface grain size of gravel bars in a braided river (Vénéon River, French Alps). Geomorphology, 285, pp. 94-105.

Wolman, M.G., 1954. A method of sampling coarse river-bed material. Trans. Am. Geophys. Union 35 (6), 951–956.

This project is co-financed by the European Regional Development Fund through the Interreg Alpine Space programme

www.alpine-space.eu/hymocares